

The Pennsylvania State University  
The Graduate School  
Department of Civil and Environmental Engineering

**EVALUATION OF CHARRED POROUS POLYMERS AS A METHOD OF  
STORM WATER POLLUTION PREVENTION FOR SHIPYARDS**

A Thesis in  
Environmental Engineering  
by  
Gordon E. Clark, Jr.

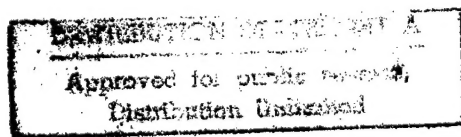
Copyright © 1998 Gordon E. Clark, Jr.

Submitted in Partial Fulfillment  
of the Requirements  
for the Degree of

Master of Science

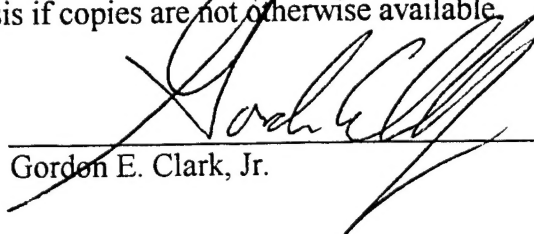
August 1998

19990202 036



**DTIC QUALITY INSPECTED 2**

I grant The Pennsylvania State University the nonexclusive right to use this work for the University's own purposes and to make single copies of the work available to the public on a not-for-profit basis if copies are not otherwise available.



---

Gordon E. Clark, Jr.

We approve the thesis of Gordon E. Clark, Jr.

Date of Signature

William D. Burgos

William D. Burgos  
Assistant Professor of Environmental  
Engineering  
Thesis Advisor

6/15/98

Brian A. Dempsey

Brian A. Dempsey  
Associate Professor of Environmental  
Engineering

6/12/98

Raymond W. Regan, Sr.

Raymond W. Regan, Sr.  
Professor of Environmental Engineering

6/12/98

Paul P. Jovanis

Paul P. Jovanis  
Professor of Civil Engineering  
Head of Department of Civil and  
Environmental Engineering

6/12/98

## ABSTRACT

Most shipyards have viable Best Management Practices (BMPs) in place to mitigate the transport of heavy metals to surface waters by storm water. Despite aggressive efforts to control storm water, shipyards have come under increased regulatory pressure to further reduce concentrations of heavy metals, such as copper and nickel, in storm water discharges. The tightening of regulatory requirements warrants research into additional BMPs. The objectives of this research project were to: (1) determine the feasibility of placing a replaceable cartridge of adsorbent material within a storm water collection system; and (2) evaluate two commercially available charred porous polymer adsorbents for the removal of heavy metals from storm water.

The results indicated that there are commercially available storm water treatment components which could be adapted to house a cartridge of porous adsorbent material. Results of the evaluation of the charred porous polymer adsorbents indicated removal effectiveness varied significantly between solute species. Whereas both charred porous polymers effectively removed  $\text{Cu}^{2+}$  from a synthetic storm water solution, neither removed  $\text{Ni}^{2+}$  effectively. Removal effectiveness also varied with the mass flow rate of the solute through the sorbent material, with mass of solute adsorbed decreasing as the mass flow rate increased. Therefore, the charred porous polymers evaluated herein can only be used to treat storm water where the solute species and mass flow rate are known and the adsorbent has demonstrated effective removal of the solute.

\_\_\_\_\_

LIST OF FIGURES.....		viii
LIST OF TABLES.....		xi
ACKNOWLEDGEMENTS.....		xii
Chapter 1	INTRODUCTION AND RESEARCH OBJECTIVES.....	1
Chapter 2	BACKGROUND.....	2
2.1	Copper and Nickel in the Aquatic Environment.....	2
2.2	Storm Water Regulations.....	3
2.3	Shipyards Practices.....	6
2.3.1	Common Shipyard Activities and Pollution Sources.....	6
2.3.2	Storm Water Best Management Practices.....	7
2.3.3	Shipyards Storm Water Collection System.....	11
2.3.3.1	Common Traits.....	11
2.3.3.2	An Example: Practical Application for Removal of Metals from Storm Water.....	12
Chapter 3	EXPERIMENTAL PROCEDURES AND MATERIALS.....	15
3.1	Overview of Test Program.....	15
3.2	Materials.....	16
3.2.1	Adsorbents.....	16
3.2.2	Synthetic Storm Water Solutions.....	17

3.2.2.1	Stock Solutions.....	17
3.2.2.1.1	Rinse and Dilution for Influent Solutions:	
	100 mM NaCl with pH Buffer.....	17
3.2.2.1.2	Dilution for Stock Solutions:	
	100 mM NaCl without pH Buffer.....	17
3.2.2.1.3	Stock Solution: 5000 mg Cu <sup>2+</sup> /L.....	18
3.2.2.1.4	Stock Solution: 10 mg Cu <sup>2+</sup> /L.....	18
3.2.2.1.5	Stock Solution: 1000 mg Ni <sup>2+</sup> /L.....	18
3.2.2.1.6	Stock Solution: 10 mg Ni <sup>2+</sup> /L.....	18
3.2.2.2	Batch Experiment Solutions.....	19
3.2.2.3	Flow Through Experiment Solutions.....	20
3.3	Experimental Methods.....	21
3.3.1	Batch Experiments.....	21
3.3.2	Flow Through Experiments.....	22
3.4	Analytical Methods.....	24
3.4.1	Atomic Absorption Spectrometry.....	24
3.4.2	AAS Calibration.....	26
3.4.2.1	Calibration Solutions for Cu <sup>2+</sup> .....	26
3.4.2.2	Calibration Solution: 1 mg Cu <sup>2+</sup> /L.....	26
3.4.2.3	Calibration Solutions for Ni <sup>2+</sup> .....	27
3.4.2.4	Calibration Solution: 0.5 mg Ni <sup>2+</sup> /L.....	27
3.5	Data Reduction.....	28

3.5.1	Batch Data Handling.....	28
3.5.2	Flow Through Data Handling.....	30
3.5.3	Freundlich Adsorption Isotherm Coefficients from Flow Through Data.....	31
Chapter 4	RESULTS AND DISCUSSION.....	37
4.1	Results.....	37
4.1.1	$\text{Cu}^{2+}$ in Synthetic Storm Water.....	37
4.1.1.1	Batch Results for $\text{Cu}^{2+}$ .....	37
4.1.1.2	Flow Through Experiment Results for $\text{Cu}^{2+}$ .....	39
4.1.1.3	Freundlich Isotherm Coefficients from Flow Through Data for $\text{Cu}^{2+}$ .....	39
4.1.2	$\text{Ni}^{2+}$ in Synthetic Storm Water.....	40
4.1.2.1	Batch Results for $\text{Ni}^{2+}$ .....	40
4.1.2.2	Flow Through Experiment Results for $\text{Ni}^{2+}$ .....	41
4.1.3	Competitive Adsorption Flow Through Results for $\text{Cu}^{2+}$ and $\text{Ni}^{2+}$ .....	41
4.2	Discussion.....	42
4.2.1	Comparison of Batch to Flow Through Experiments.....	42
4.2.2	Comparison of Adsorption of $\text{Cu}^{2+}$ to $\text{Ni}^{2+}$ .....	44
4.2.3	Comparison of Adsorption of $\text{Cu}^{2+}$ as a single solute to a bisolute system with $\text{Ni}^{2+}$ present.....	44
Chapter 5	CONCLUSION.....	54

BIBLIOGRAPHY.....	56
-------------------	----



## LIST OF FIGURES

Figure 2-1. Stormceptor <sup>TM</sup> oil/water separator plan and profile views. Under normal flow conditions storm water enters the upper chamber and flows over the weir into the lower chamber. In the lower chamber grit and sediment settle while oil and grease accumulate at the top of the baffle. The treated effluent travels up the outlet pipe, where a cartridge of adsorbent material could be located to remove dissolved metals prior to discharge. During high flows most of the storm water bypasses the lower chamber. ....	14
Figure 3-1. Elevation view of a typical adsorbent column (Snoeyink 1990). ....	34
Figure 3-2. Schematic of experimental apparatus for the flow through tests. ....	34
Figure 3-3. Single beam atomic absorption spectrometer (Fifield and Haines 1995). ....	35
Figure 3-4. Representative AAS calibration curve. ....	35
Figure 3-5. Representative time to breakthrough curve. The data shown is the triplicate data set of Supelcarb <sup>TM</sup> at an influent concentration of 5 mg Cu <sup>2+</sup> /L and constant flow rate of 300 mL/min. ....	36
Figure 3-6. Representative average time to breakthrough curve. The graph shows reduction of the triplicate data set of Supelcarb <sup>TM</sup> at an influent concentration of 5 mg Cu <sup>2+</sup> /L and constant flow rate of 300 mL/min to one average break through curve. Error bars represent the standard deviation about the mean time value. ....	36
Figure 4-1. Copper adsorption isotherm obtained with Supelcarb <sup>TM</sup> in the batch experiments. ....	46
Figure 4-2. Copper adsorption isotherm obtained with Carboxen-1011 <sup>TM</sup> in the batch experiments. ....	46
Figure 4-3. Freundlich adsorption isotherm obtained with Supelcarb <sup>TM</sup> in the batch experiments. ....	47
Figure 4-4. Copper breakthrough curves obtained with Supelcarb <sup>TM</sup> and a constant influent concentration of 5 mg Cu <sup>2+</sup> /L in the flow through experiments. Error bars represent a standard deviation about a triplicate mean. ....	48

Figure 4-5. Copper breakthrough curves obtained with Supelcarb™ and a constant flow rate of 200 mL/min in the flow through experiments. Error bars represent a standard deviation about a triplicate mean (10 mg Cu<sup>2+</sup>/L error bars no larger than symbol size).

.....48

Figure 4-6. Copper breakthrough curves obtained with Carboxen-1011™ and a constant influent concentration of 5 mg Cu<sup>2+</sup>/L in the flow through experiments. Error bars represent a standard deviation about a triplicate mean.

.....49

Figure 4-7. Copper breakthrough curves obtained with Carboxen-1011™ and a constant flow rate of 200 mL/min in the flow through experiments. Error bars represent a standard deviation about a triplicate mean.

.....49

Figure 4-8. Adsorption isotherms obtained with Supelcarb™ as calculated by the Burgisser Model for a constant influent concentration of Cu<sup>2+</sup> of 5 mg Cu<sup>2+</sup>/L in the flow through experiments.

.....50

Figure 4-9. Adsorption isotherms obtained with Supelcarb™ as calculated by the Burgisser Model for a constant flow rate of 200 mL/min in the flow through experiments.

.....50

Figure 4-10. Nickel adsorption isotherm obtained with Supelcarb™ in the batch experiments.

.....51

Figure 4-11. Nickel adsorption isotherm obtained with Carboxen-1011™ in the batch experiments.

.....51

Figure 4-12. Nickel breakthrough curves obtained with Supelcarb™ and a constant flow rate of 200 mL/min in the flow through experiments. Error bars represent a standard deviation about a triplicate mean.

.....52

Figure 4-13. Nickel breakthrough curves obtained with Carboxen-1011™ and a constant flow rate of 200 mL/min in the flow through experiments. Error bars represent a standard deviation about a triplicate mean.

.....52

Figure 4-14. Copper breakthrough in a Cu<sup>2+</sup> and Ni<sup>2+</sup> bisolute system. Curves obtained with Supelcarb™ and a constant flow rate of 300 mL/min in the flow through experiments. Error bars represent a standard deviation about a triplicate mean.

.....53

Figure 4-15. Copper breakthrough in a Cu<sup>2+</sup> and Ni<sup>2+</sup> bisolute system. Curves obtained with Carboxen-1011™ and a constant flow rate of 300 mL/min in the flow through experiments. Error bars represent a standard deviation about a triplicate mean.

.....53

## LIST OF TABLES

Table 3-1. Physical characteristics of Supelcarb™ and Carboxen-1011™. ....	16
Table 3-2. Volume of stock solution needed to make 200 mL of batch experimental solution at a desired influent concentration. ....	19
Table 3-3. Volume of stock solution needed to make 20 L of flow through experimental solution at a desired influent concentration. ....	20
Table 4-1. Summary of Freundlich adsorption isotherm coefficients for Supelcarb™ and Carboxen-1011™ from batch experiments with $\text{Cu}^{2+}$ in synthetic storm water. ....	38
Table 4-2. Summary of Freundlich adsorption isotherm coefficients for Supelcarb™ and Carboxen-1011™ from batch experiments with $\text{Ni}^{2+}$ in synthetic storm water. ....	40

## ACKNOWLEDGMENTS

The author would like to thank Dr. William D. Burgos who served as the thesis advisor for this research project. Dr. Burgos' guidance and support were crucial to the successful completion of this thesis. The author would also like to acknowledge Drs. Brian A. Dempsey and Raymond W. Regan, Sr. for serving as committee members. Thanks to John A. Kliem, LT, CEC, USN, for his patience while teaching an old dog some new tricks. A special thanks to my wife, Sandra, and our four children; Keighley, Blair, Shiona, and Aileen for their inspiration, support and love.

## Chapter 1

### INTRODUCTION AND RESEARCH OBJECTIVES

Shipyards are concentrated industrialized areas where abrasive grit blasting, painting, metal cutting, hull defouling, and machinery replacement are routine events. Two of these activities, hull defouling and painting, use the toxic effects of copper on aquatic life to remove and restrict growth of marine life, such as barnacles, on the hulls of ships. Other common activities, such as battery maintenance and welding, involve nickel-containing materials. These activities, which are often conducted outdoors, make them potential sources of heavy metal pollution of adjacent watercourses. Most shipyards have implemented substantial Best Management Practices (BMPs) to control the transport of heavy metals to receiving waters. Despite the most comprehensive and conscientious efforts to contain and collect debris, dust, and overspray, some heavy metals are transported to adjacent water bodies via the storm water collection system. The tightening of regulatory requirements, most notably National Pollution Discharge Elimination System (NPDES) permits for copper in storm water, warrants research into additional BMPs. One potential new BMP may be to place porous heavy metal adsorbents within the storm water collection system. The objectives of this research were to: (1) evaluate two commercially available carbonaceous adsorbents for the removal of heavy metals from storm water; and (2) determine the feasibility of placing a porous adsorbent within a storm water collection system.

## Chapter 2

### BACKGROUND

#### 2.1 Copper and Nickel in the Aquatic Environment

Natural processes, such as erosion and volcanic activity, introduce trace concentrations of metals into surface waterways. Many industrial activities at shipbuilding and ship repair facilities can add significant amounts of metal pollutants via storm water discharges. Improper controls on activities such as ship bottom cleaning, bilge water disposal, fuel loading and unloading, metal fabrication and cleaning operations, and surface preparation and painting provide a source of metal contaminants which can migrate to adjacent waters (Dodson 1995).

In trace concentrations, many metals, such as copper, are essential micronutrients for the maintenance of aquatic life. These metals become toxic to organisms only when levels exceed nutritional requirements (LaGrega, Buckingham, and Evans 1994). Above trace concentrations, copper becomes highly toxic to most aquatic plants, invertebrates and fish. The effects of copper toxicity to plants, such as inhibited growth, have been noted at total aqueous concentrations below 0.1 mg/L (Moore and Ramamoorthy 1984). The lethal effects concentration at which 50% of the test organisms are killed ( $LC_{50}$ ) is used as a measure of aquatic toxicity. The  $LC_{50}$  for  $Cu^{2+}$  for invertebrates and freshwater fish range between 0.017 and 1.0 mg/L (Moore and Ramamoorthy 1984). The  $LC_{50}$  for

marine fish is approximately three times higher due to the complexing capacity of saltwater and copper. For relative comparison, mercury is the only metal which is consistently more toxic to aquatic flora and fauna than copper (Moore and Ramamoorthy 1984). In contrast, nickel is one of the least toxic priority heavy metals. Nickel is not a significant or widespread contaminant of most freshwaters and marine sediments. In most industrialized parts of the world, nickel concentrations range from 1 to 3  $\mu\text{g/L}$  in unpolluted freshwater and increase to 10 to 50  $\mu\text{g/L}$  in waters from urban, industrial, sources (Moore and Ramamoorthy 1984). However, nickel and copper have been observed to act synergistically toward many species (Moore and Ramamoorthy 1984).

## **2.2 Storm Water Regulations**

The Federal Water Pollution Control Act of 1972 (FWPCA) established the basic framework of the current Clean Water Act (CWA): effluent limitation guidelines, water quality requirements, and the NPDES permit program. The act also established the Environmental Protection Agency's (EPA) responsibility to set industry specific effluent standards based on pollution control technologies and their economic feasibility. The Flannery Decree, the result of a 1976 lawsuit by environmental groups, switched the EPA's emphasis from conventional pollutants, such as Biochemical Oxygen Demand (BOD), to toxics control. The 1977 amendments to the CWA incorporated the Flannery Decree by promulgating effluent guidelines, new source performance standards, and pretreatment standards for 65 priority pollutants covering 21 major industrial categories (Adams et al. 1997). However, the significant variability of activities and pollutant sources between shipyards prevented the EPA from establishing effective limits for the

shipbuilding and repair industry. Therefore, numerical limits were set based on the regulators' Best Professional Judgement (BPJ) and Best Engineering Judgement (BEJ). The 1987 reauthorization of the CWA established a timetable for regulation of storm water, strengthened water quality related requirements, and established an "anti-backsliding policy." The "anti-backsliding policy" prohibits relaxation of BPJ standards, even if promulgated effluent guidelines establish less stringent limits (Adams et al. 1997). The act further allowed for stricter discharge limits if the technology based effluent standards failed to protect the quality of the receiving waters.

The EPA uses the NPDES program to regulate all discharges to surface waters. An NPDES permit sets numerical limits on authorized discharges, which include collected or channeled storm water (Dodson 1995). NPDES permits for storm water discharges require a storm water management plan (SWMP), which contains general, site-specific or industry specific BMPs. The objectives of SWMPs are to: (1) identify potential sources of storm water pollution; (2) describe and ensure implementation of practices to control storm water pollutants; and (3) assure compliance with the terms of the permit (Adams et al. 1997).

An example of practical application of these regulations is the BMPs most shipyards have in place to prevent grit blasting material from contacting storm water. Most shipyards shroud the blasting area to minimize the areal extent of contamination and recycle blasting material until it is unusable (Hartman Engineering, Avondale Industries, and Walk, Haydel Environmental 1997). While BMPs are integral parts of shipyard NPDES permits, numerical contaminant limits are also applied in many



instances. Numeric water quality criteria (WQC) for protecting aquatic life consist of two numbers – the Criterion Maximum Concentration (CMC) and the Criterion Continuous Concentration (CCC) (Foran 1993). The CCC represents a four day average concentration, that if exceeded more than once every three years, on average, would adversely impact aquatic organisms. The CMC represents a one hour average concentration, that if exceeded more than once every three years, on average, would adversely impact aquatic organisms (Foran 1993).

The toxicity of some substances is sometimes related to the chemical or physical characteristics of the receiving waters. For example, the toxicity of copper and nickel to aquatic life is a function of water hardness. High water hardness is accompanied by high alkalinity. Increasing the alkalinity from 50 to 250 mg/L as  $\text{CaCO}_3$ , at pH 7, increases the concentration of copper complexes, such as  $\text{CuCO}_3^0$ . Consequently, increasing the alkalinity decreases the concentration of the toxic form of copper,  $\text{Cu}^{2+}$ , from 25% to 9% of the total copper present. Therefore, increasing the water hardness decreases toxicity of dissolved copper (Snoeyink and Jenkins 1980). The effects of hardness are factored into the WQC based on the following equations (Foran 1993):

$$\text{CMC}_{\text{Cu}} = e^{(0.9422[\ln(\text{hardness})] - 1.464)} \quad (2-1)$$

$$\text{CCC}_{\text{Cu}} = e^{(0.8545[\ln(\text{hardness})] - 1.465)} \quad (2-2)$$

$$\text{CMC}_{\text{Ni}} = e^{(0.846[\ln(\text{hardness})] + 3.361)} \quad (2-3)$$

$$\text{CCC}_{\text{Ni}} = e^{(0.846[\ln(\text{hardness})] + 1.165)} \quad (2-4)$$

where (LaGrega, Buckingham, and Evans 1994):

CMC = Criterion Maximum Concentration ( $\mu\text{g M}^{2+}/\text{L}$ )

CCC = Criterion Continuous Concentration ( $\mu\text{g M}^{2+}/\text{L}$ )

hardness = measured hardness as mg/L as  $\text{CaCO}_3$ .

The proposed 1995 amendments to the CWA included: (1) extended compliance deadlines for discharge limitation, up to three years, for implementing innovative pollution prevention technologies, process or recycling methods; and (2) clarified what constitutes increases in loading (Hartman Engineering, Avondale Industries, and Walk, Haydel Environmental 1997). As of May 1998, these amendments have yet to be enacted into law.

## **2.3 Shipyard Practices**

### **2.3.1 Common Shipyard Activities and Pollution Sources**

Following a survey of 16 shipyards, covering a variety of locations, missions, and capacities, Hartman Engineering et al. (1997) reported that the shipyard process areas most commonly affected by the CWA are dry docks, graving docks, painting facilities, railways and maintenance facilities.

While process areas may vary, the literature suggests common activities occurring at these areas are the primary concern of potential sources of metal contaminated storm water. Activities such as ship bottom cleaning (abrasive and chemical defouling), bilge water disposal, loading and unloading of fuels, metal fabrication and cleaning, and surface preparation and painting (Dodson 1995), machinery component replacement and boiler rehabilitation generate spent solvents and waste oils containing metal leachate (Manning 1995) and metal particulates.

The Applied Research Laboratory at Pennsylvania State University (ARL) reported in a 1997 survey of 30 shipyards that the processes that were generally considered the biggest sources of pollution were surface preparation, coating and cleaning (Applied Research Laboratory 1997). Similarly, Ross (1993) and Host (1996) each reported that the most significant sources of pollutants from dry docks and graving docks came from heavy metals in spent abrasives, chips from antifoulant paints, and spills and overspray of antifoulant paint.

These potential sources of storm water contaminants are well documented and widely recognized throughout the shipbuilding and repair industry. However, for these contaminant sources to become problematic, a pathway must exist for the transport to the receiving waters by the storm water runoff. A pathway for contaminant transport exists in the storm water collection system.

### **2.3.2 Storm Water Best Management Practices**

Unlike traditional NPDES permit requirements, EPA general permits for storm water do not require treatment but instead emphasize BMPs that reduce discharges at the source. In general, once the process of identifying and assessing sources of storm water discharges is complete, the shipyards must evaluate and select the pollution prevention measures, BMPs and other controls that will be implemented. BMPs include processes, procedures, schedules of activities, prohibitions on practices and other management practices that prevent or reduce the discharge of pollutants in storm water run off. BMPs typically emphasize source control measures, such as material segregation, water

diversion and dust control. Where these measures are not practical or effective, BMPs focus on preventive maintenance, chemical substitution, spill prevention, good housekeeping, training, recycling and lastly, treatment of storm water (Dodson 1995).

Overall, shipyards employ aggressive and comprehensive BMPs to prevent metal contaminants from entering storm waters. For example, Puget Sound Naval Shipyard's (PSNS) BMP plan includes schedules of activities, prohibitions on practices, maintenance procedures, and other management practices to prevent or reduce pollution into waters of Sinclair Inlet. The PSNS BMPs also include treatment requirements, operating procedures, and practices to control site runoff, spill or leaks, waste disposal or drainage from raw material.

The literature (e.g., Hartman Engineering et al. 1997; Host 1996; and Ross 1993) clearly shows that the shipyards consider spent abrasives and paint chips their primary concern for compliance with storm water discharge permits. Shipyards' BMPs emphasize preventing spent abrasives and paint chips from becoming airborne and settling directly on the surface waters or lying on the dry dock floor where metals may leach out. In addition, Hartman Engineering et al. (1997) reported that most shipyards had BMPs to control storm water discharges that contact pollutants that included collecting storm water in drums for on-site treatment or hazardous waste disposal. Other measures, as reported by Host (1996), include daily cleaning of abrasive blasting and paint to a "residue free" standard and enclosures of heavy, water proof, plastic coated, canvas for temporary, exterior paint and grit blasting enclosures. Ross (1993) reiterated these BMPs, though in more general terms, in a list of ten recommended BMPs for dry

docks and graving docks. Four of ten recommended controls specifically addressed controlling contact with, and contamination of, storm water by spent paint and abrasive blasting material (Ross 1993). Other BMPs addressed housekeeping, maintenance and spill response.

The area of controlling pollution from surface preparation and painting is significant enough to warrant the National Shipbuilding Research Program (NSRP) funding research into current and future technologies that reduce air emissions and water discharges. The research by the ARL (1997) included literature reviews and surveys on pollution prevention and control strategies for surface preparation, surface coating, and water treatment. In the wake of their survey, ARL recommended the following technologies: ultra-high pressure water blasting (UHP), utilizing recycled water it inherently controls dust and leaves no spent abrasives; the Sponge-Jet®, a sponge particle with abrasive aggregate which is recyclable and produces 94% less dust than traditional abrasive blasting; and Cryogenic Carbon Dioxide (CO<sub>2</sub>) Pellet Blasting, a solid pellet of CO<sub>2</sub> (dry ice) striking the surface as an abrasive but generating a small amount of waste since the pellets volatilizes leaving only the removed coating.

Regardless of the method of surface preparation, all respondents reported employing enclosures, either around the blasting operation or around the entire dry dock. One interesting recommendation by ARL (1997) was for the Compliant All Position Enclosure (CAPE). The CAPE is an enclosure that secures to the ship's hull and captures emissions from blast cleaning and painting. The air emissions are then circulated to a fully self-contained barge where they are filtered, dehumidified, and heated. The treated

air is then returned to the enclosure for reuse. In addition to enclosures, most shipyards reported using low volatile organic compound (VOC) coatings and airless or air-assisted airless paint guns.

Finally, ARL (1997) identified three potential treatment methods for storm water. ARL recommended sand filters and wet detention ponds, primarily for removal of BOD, hydrocarbons and sediments. Sand filters and wet detention ponds normally require a substantial investment in land. Shipyards typically are located in areas of concentrated land use and have very limited amounts of land available for this type of use. The third technology identified was vortex solids separators, which have demonstrated effectiveness for removal of solids and floatables.

As demonstrated in the literature, the shipyards expend considerable effort to minimize contact between rainwater and spent abrasives to prevent contamination of storm water. The significance of these efforts was highlighted by Gauthier et al. (1996) in a report to the Naval shipyards that recommended avoiding treating storm water for copper because of the high initial cost, up to \$400 million, and high annual cost, nearly \$90 million. The report by Gauthier et al. (1996) was based on a system of lime precipitation and reverse osmosis for an annual flow of 125 million gallons per day (MGD). By comparison, PSNS reported flows of 7 MGD from their system of six dry docks. Therefore, if the costs reported by Gauthier et al. (1996) are proportionate to daily flow capacity then the initial annual costs for a treatment system would be \$22.4 million and \$5.04 million, respectively, for PSNS.

### **2.3.3 Shipyard Storm Water Collection System**

#### **2.3.3.1 Common Traits**

Most shipyards were constructed when it was acceptable practice to discharge process wastewater and sanitary wastes directly into adjacent water. As environmental regulations have restricted these practices, the shipyards have altered and cross-connected the piping systems to redirect wastes into sanitary sewers. These reconnections have created a complex maze of sometimes old, corroded, and broken underground pipes (Gauthier et al. 1995). Cracked and broken underground pipes can lead to ground water intrusion, which could increase the volume of storm water discharges and carry additional contamination to receiving waters. This situation has significant financial implications on the cost of complying with discharge permits. For example, at the Pearl Harbor Naval Shipyard, dissolved nutrients and free-phase and dissolved oil seep into the storm water sewer, contaminate the storm water and require additional treatment. PSNS and Norfolk Naval Shipyard also experience groundwater intrusion into their storm sewer system. However, these two locations do not have groundwater contaminants and therefore potentially serve to dilute contaminant concentrations (Gauthier et al. 1995).

Saltwater intrusion is also a common characteristic of shipyard storm sewers. Saltwater intrusion, primarily from tidal influences, results in brackish water mixing with storm water and changing the physical properties of the effluent, most notably the ionic strength and pH. Gadbois (1997) reported findings of saltwater intrusion at the San

Diego Naval Station. Likewise, Gauthier et al. (1995) reported similar findings for PSNS and for the Portsmouth Naval Shipyard.

The engineering literature provides few details on specific configurations of storm water collection systems typically encountered at a commercial or Naval shipyard. However, a mix of combined sewers, sanitary sewers, and separate sewers would be expected. PSNS's storm water BMPs provide the best insight into the types of drainage systems currently employed. Dry docks floors are equipped with cross-drains and gutters to channel runoff from the floor into side tunnels, leading to the main drainage tunnel and pump wells. Several of the dry docks are linked by a single drainage tunnel to a pump well that discharges to an outfall. The majority of water handled by this system, over 7 MGD, comes from controlling the hydrostatic pressure against the dry dock walls. Other sources of water, such as caisson leaks, gate leakage, storm water, potable water, steam condensate and non-contact cooling water, add to the volume of water handled by the drainage system. The dry dock Process Water Collection Systems (PWCS) collect storm water runoff from the dry dock floor. This system for collecting and routing storm water to the sanitary sewer, portable storage tanks or the receiving waters allows the shipyard to minimize its permit violations by determining the routing based on the level of contaminant.

#### **2.3.3.2 An Example: Practical Application for Removal of Metals from Storm Water**

The primary components of storm water collection systems include the: (1) storm drains and inlets; (2) pipe network; (3) flow collection and treatment; and (4) the outfall.



Treatment devices, such as oil/water separators and sedimentation basins represent the most logical and cost effective location to attempt in-line treatment for dissolved metals, such as a cartridge of porous adsorbent material. Standard manholes, pipes or weirs would not be sufficient because the direct flow can carry particulates and debris that could foul or dislodge an adsorbent cartridge.

Commercially available baffled sedimentation basins such as those produced by Vortech<sup>TM</sup> and Stormceptor<sup>TM</sup>, (Figure 2-1), remove suspended solids, trap oil, and allow high flow by-pass. The Stormceptor<sup>TM</sup> diverts storm water flow into a treatment chamber through a weir and inlet pipe. The inlet pipe directs water tangentially along the treatment chamber wall, where sediment settling occurs due to gravity and centrifugal force (Stormceptor 1996). The submerged entrance of the outlet pipe causes entrapment of floatable solids and liquids with specific gravity less than water, such as oil. The treated water flows up through the outlet pipe into the by-pass chamber, downstream of the weir. Under high flow conditions, the weir directs the water past the inlet pipe, into the by-pass chamber, and out of the device. The outlet pipe from the Stormceptor<sup>TM</sup> treatment chamber could be retrofitted with a replaceable cartridge of porous adsorbent material to capture dissolved metals.

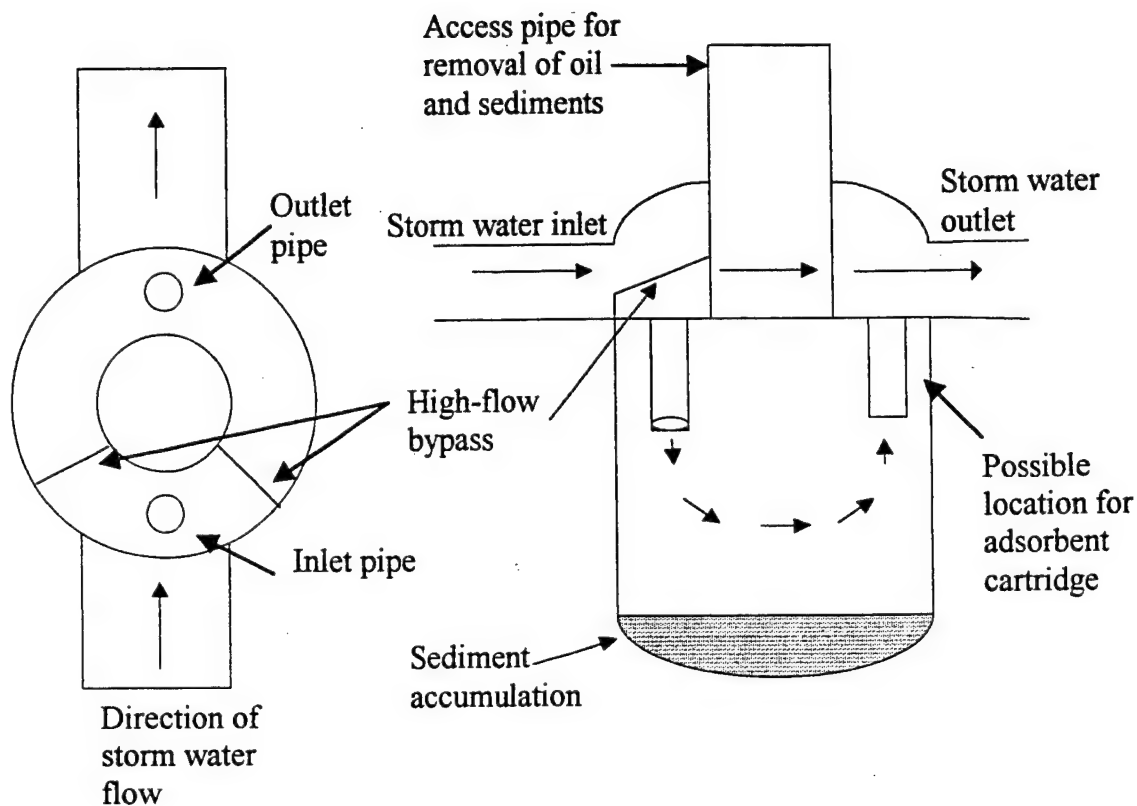


Figure 2-1. Stormceptor™ oil/water separator plan and profile views. Under normal flow conditions storm water enters the upper chamber and flows over the weir into the lower chamber. In the lower chamber grit and sediment settle while oil and grease accumulate at the top of the baffle. The treated effluent travels up the outlet pipe, where a cartridge of adsorbent material could be located to remove dissolved metals prior to discharge. During high flows most of the storm water bypasses the lower chamber.

## Chapter 3

### EXPERIMENTAL PROCEDURES AND MATERIALS

#### 3.1 Overview of Test Program

Experiments were conducted to measure the adsorbent capacity and contaminant breakthrough characteristics of copper ( $\text{Cu}^{2+}$ ) and nickel ( $\text{Ni}^{2+}$ ) using two carbonaceous, charred porous polymer adsorbents, Supelcarb<sup>TM</sup> and Carbonex-1011<sup>TM</sup> (Supelco, Inc., Bellefonte, PA). The adsorbents have nearly identical physical properties (e.g., surface area, particle size and density) and essentially vary only in pore shape and pore size distribution. Batch adsorption experiments were conducted with both adsorbents to determine adsorption isotherms for  $\text{Cu}^{2+}$  and  $\text{Ni}^{2+}$  in a synthetic brackish storm water solution of 100 mM NaCl, adjusted to pH  $6.3 \pm 0.2$  with 100 mM  $\text{Na}(\text{HCO}_3)_2$ . Flow through experiments, used to determine breakthrough characteristics, involved pumping synthetic storm water solutions containing single solute  $\text{Cu}^{2+}$  or  $\text{Ni}^{2+}$ , or bisolute  $\text{Cu}^{2+}$  and  $\text{Ni}^{2+}$  through an adsorbent cartridge (2.06 cm diameter, 7.8 cm bed depth) at bed velocities expected within a storm water collection system. Influent and effluent concentrations were measured using atomic absorption spectrometry (AAS). Experimental variables included influent metal concentration (2.5 to 10 mg/L for  $\text{Cu}^{2+}$  and 1.25 to 5 mg/L for  $\text{Ni}^{2+}$ ) and flow rate (100 to 300 mL/min).

### 3.2 Materials

#### 3.2.1 Adsorbents

Adsorbents used in this experiment were charred porous polymers, Supelcarb<sup>TM</sup> and Carboxen-1011<sup>TM</sup>, manufactured by Supelco, Inc. of Bellefonte, PA. The adsorbents were selected for their unique pore shapes and pore size distribution. Supelcarb<sup>TM</sup> is characterized by "dead end" pores; pores, which are funnel shaped and do not transfix the particle's core. Carboxen-1011<sup>TM</sup> adsorbent pores pierce the particle's core in an "hour glass" shape. Physical characteristics of the two adsorbents are listed in Table 3-1.

Table 3-1. Physical characteristics of Supelcarb<sup>TM</sup> and Carboxen-1011<sup>TM</sup>.

Adsorbent	Shape	Diameter ( $\mu\text{M}$ )	Bulk Density (g/cc)	Porosity		
				Micro ( $<10\mu\text{M}$ )	Meso (10– 100 $\mu\text{M}$ )	Macro ( $>100\mu\text{M}$ )
Supelcarb <sup>TM</sup>	sphere	400–800	0.46	0.37	0.25	0.27
Carboxen– 1011 <sup>TM</sup>	sphere	400–800	0.44	0.42	0.19	0.27

### **3.2.2 Synthetic Storm Water Solutions**

All experiments used a synthetic storm water of 100 mM NaCl to maintain constant ionic strength. All synthetic storm water solutions were buffered with 100 mM  $\text{NaHCO}_3$ . The pH was adjusted with 100 mM NaOH or 100 mM HCl. The procedures used are outlined below:

#### **3.2.2.1 Stock Solutions**

##### **3.2.2.1.1 Rinse and Dilution for Influent Solutions: 100 mM NaCl with pH Buffer**

1. Weigh out 116.886 g of "Ultra Pure" NaCl (J.T. Baker) on a Delta Range® Mettler Balance, Model AG204;
2. measure 50 mL of 100 mM  $\text{Na}(\text{HCO}_3)_2$  (Fisher Scientific) in a class A, volumetric flask and place into an acid washed 28 L Nalgene™ container, as a pH buffer;
3. dissolve the NaCl with 4 L of de-ionized water in a 4 L Ehrlenmyer flask;
4. pour the solution into the Nalgene™ container;
5. use the 4 L Ehrlenmyer Flask to add 16 L of de-ionized water; for a total of 20.05 L, 100 mM NaCl.

##### **3.2.2.1.2 Dilution for Stock Solutions: 100 mM NaCl without pH Buffer**

1. Weigh out 116.886 g of "Ultra Pure" NaCl (J.T. Baker) on a Delta Range® Mettler Balance, Model AG204;
2. dissolve the NaCl with 4 L of de-ionized water in a 4 L Ehrlenmyer flask;
3. pour the solution into the Nalgene™ container;
4. use the 4 L Ehrlenmyer Flask to add 16 L of de-ionized water; for a total of 20 L, 100 mM NaCl.

**3.2.2.1.3 Stock Solution: 5000 mg Cu<sup>2+</sup>/L**

1. In an acid washed 1000 mL, class A, volumetric flask, add 5 mL of 50% Nitric Acid (VWR) (1 + 1 HNO<sub>3</sub>) as a preservative;
2. weigh out 13.4107 g of CuCl<sub>2</sub>•2H<sub>2</sub>O (Fisher Scientific) on a Delta Range® Mettler Balance, Model AG204;
3. add the 13.4107 g of CuCl<sub>2</sub>•2H<sub>2</sub>O to the flask;
4. dilute to 1000 mL with unbuffered stock dilution solution.

**3.2.2.1.4 Stock Solution: 10 mg Cu<sup>2+</sup>/L**

1. Pipette one milliliter of 5000 mg Cu<sup>2+</sup>/L stock solution into an acid washed, 500 mL, class A, volumetric flask;
2. fill to 500 mL with buffered stock dilution solution.

**3.2.2.1.5 Stock Solution: 1000 mg Ni<sup>2+</sup>/L**

1. In an acid washed 1000 mL, class A, volumetric flask, add 5mL of 50% Nitric Acid (VWR) (1 + 1 HNO<sub>3</sub>) as a preservative;
2. weigh out 4.0472 g of "Baker Analyzed®" NiCl<sub>2</sub>•6H<sub>2</sub>O (J.T. Baker) on a Delta Range® Mettler Balance, Model AG204;
3. add the 4.0472 g of NiCl<sub>2</sub>•6H<sub>2</sub>O to the flask;
4. dilute to 1000 mL with unbuffered stock dilution solution.

**3.2.2.1.6 Stock Solution: 10 mg Ni<sup>2+</sup>/L**

1. Pipette 5 mL of 1000 mg Ni<sup>2+</sup>/L stock solution into an acid washed, 500 mL, class A, volumetric flask;
2. fill to 500 mL with buffered stock dilution solution.

### 3.2.2.2 Batch Experiment Solutions

1. For the desired influent concentration, the amount shown in Table 3-2, was added to an acid washed, 200 mL, class A volumetric flask;

Table 3-2. Volume of stock solution needed to make 200 mL of batch experimental solution at a desired influent concentration.

Metal Ion Concentration (mg $M^{2+}/L$ )	Volume of 10 mg $Cu^{2+}/L$ (mL)	Volume of 5000 mg $Cu^{2+}/L$ (mL)	Volume of 10 mg $Ni^{2+}/L$ (mL)	Volume of 1000 mg $Ni^{2+}/L$ (mL)
1.25	25	0	25	0
2.5	50	0	50	0
5	100	0	100	0
10	200	0	200	0
25	0	1	0	5
50	0	2	0	10
100	0	4	0	20

2. add buffered stock dilution solution until approximately two-thirds full;
3. check pH with a Beckman  $\phi$  31 pH meter and adjust to pH of  $6.3 \pm 0.2$  with 100 mM  $Na(HCO_3)_2$  (Fisher Scientific);
4. fill to 200 mL with buffered stock dilution solution.

### 3.2.2.3 Flow Through Experiment Solutions

1. For the desired influent concentration, the amount shown in Table 3–3 was added to an acid washed, 20 L, Nalgene™ container;

Table 3–3. Volume of stock solution needed to make 20 L of flow through experimental solution at a desired influent concentration.

Experimental Concentration (mg Cu <sup>2+</sup> /L)	Experimental Concentration (mg Ni <sup>2+</sup> /L)	Volume of 5000 mg Cu <sup>2+</sup> /L (mL)	Volume of 1000 mg Ni <sup>2+</sup> /L (mL)	Mass of NiCl <sub>2</sub> •6H <sub>2</sub> O (grams)
2.5	0	10	0	0
5.0	0	20	0	0
10.0	0	40	0	0
0	1.25	0	25	0
0	2.0	0	40	0
0	5.0	0	100	0
5	4.62	20	0	0.3740
10	4.62	40	0	0.3740
5	9.24	20	0	0.7479

2. fill to 20 L with buffered stock dilution solution;
3. check pH with a Beckman ø 31 pH meter and adjust to pH of 6.3 ± 0.2 with 100 mM Na(HCO<sub>3</sub>)<sub>2</sub> (Fisher Scientific).



### **3.3 Experimental Methods**

All experiments described below were conducted in triplicate to balance statistical reliability, budget and schedule restrictions.

#### **3.3.1 Batch Experiments**

Batch experiments were conducted to evaluate adsorption isotherms for  $\text{Cu}^{2+}$  and  $\text{Ni}^{2+}$  at a constant ionic strength of 0.1 mM to simulate a tidal washed storm sewer environment. The experiment involved a 250 mL beaker as a reactor vessel containing 200 mL of the metal spiked synthetic storm water solution, and 1 gram (dry weight) of adsorbent. Once combined, the reactor contents were continuously mixed, using a Teflon™ magnetic stir bar on a Challenge Environmental Systems, Model MS8-300, 8-position magnetic stirring plate, for ten minutes. Ten minute contact time was selected to approximate the maximum residence time of storm water in an adsorbent column during a low – flow storm event. After ten minutes, the adsorbent and solution were separated using a 0.45 µm Analytical Filter Unit (Nalgene™, CN, Model 130-4045). The pH of the solution was adjusted to less than 2.0 by adding one to two drops of concentrated nitric acid. The influent and effluent concentrations were measured using a Perkin-Elmer™, Model 3030 B, Atomic Absorption Spectrometer (AAS). The procedures used are outlined below:

1. Prepare in triplicate the eight influent concentrations (Table 3-2) in separate 250 mL beakers;
2. remove 1 mL from each reactor and place in separate, acid washed, 25 mL, class A, volumetric flasks;

3. to each 25 mL flask add one drop of concentrated nitric acid;
4. fill with buffered stock dilution solution and set aside;
5. in the remaining 250 mL reactors, place an acid washed Teflon™ magnetic stir bar and place on a Challenge Environmental Systems, Model MS8-300, 8-position magnetic stirring plate;
6. to each reactor, add 1 gram of adsorbent (previously weighed on a Delta Range® Mettler Balance, Model AG204) and let mix for ten minutes;
7. after ten minutes, separate the adsorbent from the solution using a 0.45µm Analytical Filter Unit (Nalgene™, CN, Model 130-4045);
8. measure the pH of each filtered solution with a Beckman ø 31 pH meter;
9. add one to two drops of concentrated nitric acid (VWR) to eight clean, acid washed, 250 mL beakers;
10. place the filtered solution from each sample in separate beakers;
11. measure the pH in each beaker, with a Beckman ø 31 pH meter, to ensure it is below 2.0;
12. measure the influent and effluent concentrations using the AAS.

### **3.3.2 Flow Through Experiments**

Flow through experiments were conducted to determine the effects of varying mass flow rates on sorption and contaminant breakthrough. Influent solutions, of varying metal concentration, were pumped at constant flow rates through an in-line 0.45 µm filter (Gelman™, Model 12178) and a one-inch diameter column containing  $12.0 \pm 0.1$  grams of tightly packed adsorbent (Figure 3-1).

The column discharged to two mixing basins in series. The first basin served as a port to monitor outlet pH. The second basin served as a mixing port for a slow continuous titration of concentrated nitric acid to maintain pH less than 2.0 and as a sampling port where concentrations could be measured by AAS at one minute intervals. "Breakthrough" was defined as the point where the effluent concentration equaled 10% of the influent concentration. Once the 10% criteria was attained, the influent was switched to a rinse of metal free synthetic storm water solution for ten minutes. Measurements were taken every minute during rinsing to evaluate if any desorption occurred. The procedures used are outlined below:

1. Cut a six inch length of one inch O.D. stainless steel tube ( $1\frac{3}{16}$  inch I.D.) and fit one end with Swagelok™ reducing unions from 1 inch to  $\frac{3}{8}$  inch;
2. using a  $\frac{1}{2}$  inch stainless steel rod, pack the column with approximately  $\frac{1}{2}$  inch of glass wool;
3. weigh out  $12.0 \pm 0.1$  g of adsorbent on a Delta Range® Mettler Balance, Model AG204;
4. pour 25% of the adsorbent into the column;
5. compact the adsorbent by "rodding" it 24 times with the stainless steel rod;
6. repeat steps 4 and 5 three more times;
7. tightly pack the remainder of the column with glass wool;
8. close the column with another set of Swagelok™ reducing unions from 1 inch to  $\frac{3}{8}$  inch;
9. set up experimental apparatus as shown in Figure 3-2;

10. prepare 20 L of rinse solution;
11. prepare 20 L of metal-spiked synthetic storm water solution (Table 3-3);
12. measure the concentration of metal ions in the influent by AAS;
13. pump metal-free rinse until the desired flow rate (100, 200, or 300 mL/min) is achieved, using the Master Flex® L/S™ Variable-Speed Modular Drive with L/S™ 18 pump head;
14. adjust the concentrated nitric acid (VWR) “drip” to maintain pH <2 in the sampling basin;
15. place the AAS aspirator at the outlet of the sampling basin;
16. switch inlet flow from rinse to spiked influent solution;
17. start timer;
18. take initial AAS reading;
19. take AAS readings at one minute intervals;
20. when AAS readings indicate effluent concentration  $\geq 10\%$  of influent, switch influent back to rinse;
21. continue rinse for ten minutes or until effluent concentration returns to zero.

### **3.4 Analytical Methods**

#### **3.4.1 Atomic Absorption Spectrometry**

Metal ion concentrations were measured on a Perkin-Elmer™, Model 3030 B, AAS, with a Perkin-Elmer™, PR-100 Printer for data capture. AAS utilizes absorption of ultraviolet or visible radiation to determine the concentration of samples. The schematic diagram of the AAS is shown in Figure 3-3.

At the light source, an electric potential is introduced between the cathode and the anode, energizing a hollow cathode lamp consisting of an anode and a metal specific cathode. The potential difference causes electrons to strike the cathode, resulting in "sputtered" metal ions, some with electrons elevated to "excited" orbitals. The excited electrons fall back into the "ground state", sending light at a unique wavelength,  $\pm 0.01\text{nm}$ , through the flame which contains sample metal ions in the ground electron state. The light source is mechanically chopped to create a double beam, one beam passing through the flame and the other around the flame.

A small portion of the sample is aspirated into the flame. This sample is made into an aerosol and then converted to gaseous elementary particles. This process is referred to as vaporization. The vaporized sample will absorb light in direct proportion to its concentration. The remaining light will pass to the monochromator, dispersing it and sending a specific wavelength of light to the detector. The detector will convert the light it absorbs into an electronic signal. The auto calibration feature on this machine will take the absorbance reading and apply it to a standard curve of absorbance versus concentration. The concentration can now be viewed on the AAS computer screen.

All samples were filtered, using a  $0.45\ \mu\text{m}$  filter, then acidified to a  $\text{pH} < 2.0$  in accordance with Standard Methods, 313A for  $\text{Cu}^{2+}$  and 321 for  $\text{Ni}^{2+}$  (APHA 1985). Acidification prevents the metal from adsorbing to the sides of the container, as metals are more soluble at low pHs. Additionally, acidification dissolves most  $\text{Cu}^{2+}$  and  $\text{Ni}^{2+}$  precipitates, especially oxy-hydroxides and carbonates.

### **3.4.2 AAS Calibration**

The AAS required calibration prior to measuring the influent and effluent concentrations in each experiment. The AAS was calibrated by comparing solutions of known concentration and ionic strength to the measured absorbance. Calibration solutions were sampled during the course of each experiment, and at the conclusion of each run, to check the accuracy of the AAS.

Within a limited range, the AAS measured absorbance is directly proportional to the concentration. The concentration can be derived from the slope ( $m$ ) and intercept ( $b$ ) of the calibration curve. The calibration curve compares measured absorbance against known concentrations. The AAS allows the operator the option to auto-zero the instrument to establish a benchmark reading from which all subsequent readings are relative. The auto-zero function was utilized for the 0 mg/L calibration solution. Therefore, the value of the y intercept ( $b$ ) is 0 for every calibration curve. Figure 3-4 is a representative calibration curve and shows the constants for calculating experimental concentrations from measured absorbances.

#### **3.4.2.1 Calibration Solutions for $\text{Cu}^{2+}$**

The AAS was calibrated using solutions of: 0, 1, 2, 3, 4 and 5 mg  $\text{Cu}^{2+}$ /L. The procedure is described below:

#### **3.4.2.2 Calibration Solution: 1 mg $\text{Cu}^{2+}$ /L**

1. In an acid washed 1000 mL, class A, volumetric flask, add 5 mL of 50% Nitric Acid (VWR) (1 + 1  $\text{HNO}_3$ ) as a preservative;
2. pipette 1 mL of 1000 mg/L Atomic Absorption Standard (E.M. Scientific);

3. weigh out 5.8443 g of "Ultra Pure" NaCl (J.T. Baker) on a Delta Range® Mettler Balance, Model AG204;
4. add the 5.8443 g of "Ultra Pure" NaCl (J.T. Baker) to the flask;
5. dilute to 1000 mL with Milli-Q™ de-ionized water (Millipore);
6. repeat steps 1 through 5 four times, each time increasing the volume of Atomic Absorption Standard by 1 mL.
7. repeat steps 1 through 5, omitting step 2, to make the 0 mg  $\text{Cu}^{2+}$ /L calibration solution.

#### **3.4.2.3 Calibration Solutions for $\text{Ni}^{2+}$**

The AAS was calibrated using solutions of: 0, 0.5, 1, 1.5, and 2 mg  $\text{Ni}^{2+}$ /L. The procedure is described below:

#### **3.4.2.4 Calibration Solution: 0.5 mg $\text{Ni}^{2+}$ /L**

1. In an acid washed 200 mL, class A, volumetric flask pipette 1 mL of 1000 mg/L Atomic Absorption Standard (J.T. Baker);
2. dilute to 200 mL with unbuffered stock solution dilution to make a 5 mg  $\text{Ni}^{2+}$ /L solution;
3. In an acid washed 1000 mL, class A, volumetric flask, add 5 mL of 50% Nitric Acid (VWR) (1 + 1  $\text{HNO}_3$ ) as a preservative;
4. add 100 mL of 5 mg  $\text{Ni}^{2+}$ /L;
5. weigh out 5.8443 g of "Ultra Pure" NaCl (J.T. Baker) on a Delta Range® Mettler Balance, Model AG204;
6. add the 5.8443 g of "Ultra Pure" NaCl (J.T. Baker) to the flask;

8. dilute to 1000 mL with Milli-Q™ de-ionized water (Millipore);
9. for the 1.5 mg Ni<sup>2+</sup>/L solutions, repeat steps 1 through 6, increasing the volume of Atomic Absorption Standard in step 1 to 3 mL.
10. for the 1 and 2 mg Ni<sup>2+</sup>/L solutions, follow the procedure outlined in section 3.4.2.2, substituting AAS Nickel Standard for Copper.
11. repeat steps 3 through 7, omitting step 4, to make the 0 mg Ni<sup>2+</sup>/L calibration solution.

### **3.5 Data Reduction**

Data captured from an experiment, in the form of measured absorbances (MA), were converted to experimental concentrations using the following formula:

$$C = m * MA + b \quad (3-1)$$

where:

C = concentration of metal ions on a mass per volume basis,

m = slope of the calibration curve,

MA = AAS measured absorbance of sample,

b = y intercept of the calibration curve (= 0 due to auto-zero feature of AAS).

Once the influent and effluent concentrations were calculated, the data were reduced to their reported form depending on the test type, batch or kinetic. The procedures for handling data from both types of experiments are described below:

#### **3.5.1 Batch Data Handling**

1. Subtract the final concentration from the initial,

$$C_8 = C_i - C_f \quad (3-2)$$



where:

$C_{\delta}$  = concentration of metal ions removed (mg/L),

$C_i$  = initial concentration of metal ions (mg/L),

$C_f$  = final concentration of metal ions (mg/L);

2. multiply the difference in concentrations by the volume of solution to get mass of metal ions removed:

$$M_{\delta} = C_{\delta} * V \quad (3-3)$$

where:

$M_{\delta}$  = mass of metal ions removed (mg),

$C_{\delta}$  = concentration of metal ions removed (mg/L),

$V$  = volume of solution (L);

3. divide the mass of metal ions removed by the mass of adsorbent in the reactor:

$$S = M_{\delta} \div M_{ads} \quad (3-4)$$

where:

$S$  = mass of metal ions sorbed per mass of adsorbent (mg  $M^{2+}$ /g adsorbent),

$M_{ads}$  = mass of adsorbent in the reactor (g);

4. plot the final concentration of metal ions ( $C_f$ ) versus sorbed concentration ( $S$ );
5. calculate  $K_f$  and  $n$  using the Freundlich Equation (Schwarzenbach, Gschwend, and Imboden 1993):

$$S = K_f * C_f^n \quad (3-5)$$

where:

$C_f$  = dissolved concentration (mg  $M^{2+}$ / L),

$K_f$  = Freundlich distribution coefficient  $(L/g)^{1/n}$ ,

$n$  = Freundlich measure of non-linearity.

The capacity of the adsorber is described by  $K_f$ . The term  $n$  describes the strength of the adsorption bond. For example, when  $K_f$  and  $C_f$  are held constant, decreasing values of  $n$  have a reduced effect on  $S$ . Smaller values of  $n$  represent stronger adsorption bonds and increased irreversibility of the reaction. Likewise, larger values of  $n$  indicate weaker adsorption bonds and increase the sensitivity of  $S$  to small changes in  $C_f$  (Snoeyink 1990). For these reasons, the Freundlich adsorption isotherm constants provide a practical basis for evaluating the performance of an adsorbing media.

### **3.5.2 Flow Through Data Handling**

1. Divide the effluent concentrations by the influent concentration to get the ratio of effluent to influent concentration;

$$C_i \div C_f = C_\alpha \quad (3-6)$$

2. plot the time to breakthrough, time ( $t$ ) vs. the effluent ratio ( $C_\alpha$ ), through  $C_\alpha = 0.10$ ;
3. from the graph determine the times for each experiment to reach  $C_\alpha = 0.02, 0.04, 0.06, 0.08$  and  $0.10$ ;
4. average the times for the three experiments and develop a composite time to breakthrough curve;
5. in experiments where an effluent ratio is observed at more than one time, the averaged value is used for the composite graph;
6. Figures 3-5 and 3-6 illustrate the procedure outlined above.

### 3.5.3 Freundlich Adsorption Isotherm Coefficients from Flow Through Data

The breakthrough characteristics measured in the flow through experiments were used to estimate adsorption isotherm coefficients. Transport and sorption of a contaminant in porous media can be represented as (Schnoor 1996):

$$\frac{\partial c}{\partial t} = -U_x \frac{\partial c}{\partial x} + D_x \frac{\partial^2 c}{\partial x^2} - \frac{\partial S}{\partial t} \frac{\rho_b}{\theta} \quad (3-7)$$

where:

$U_x$  = Darcy velocity (cm/sec),

$D_x$  = contaminant diffusivity in water (cm<sup>2</sup>/sec),

$\rho_b$  = bulk density of the porous medium (mg/cm<sup>3</sup>), and

$\theta$  = effective porosity (dimensionless).

For column experiments of the size and magnitude reported here, the effects of dispersion can be neglected (Liu and Weber 1981). As long as local equilibrium is achieved and by neglecting dispersion, the breakthrough curve can be integrated to calculate the corresponding sorbed concentration by (Burgisser et al. 1993):

$$S = \frac{1}{\rho} \int_0^c \left( \frac{t(c')}{t_0} - 1 \right) dc' \quad (3-8)$$

where:

$t(c')/t_0$  = the pore volumes eluted at concentration  $c'$  and

$\rho$  = density of the fluid in the column, ( $\rho_b/\theta$ ).

At equilibrium, where influent entering the adsorber bed equals the effluent concentration, the adsorber becomes ineffective as a method of treating for dissolved metals. Since the purpose of this experiment was to determine the feasibility of using a charred porous polymer to remove dissolved metals from storm water, a breakthrough, or

useful life, criteria was established at 10% of the influent concentration. The literature reviewed for this research (e.g., Ong and Swanson 1966; Sag and Kutsal 1995) based reported results, such as  $K_f$  and  $n$ , on experiments conducted until equilibration, where the effluent concentration equaled the influent concentration, was reached. For this reason, comparison of adsorber performance in experiments where the experimental endpoint condition is something other than complete breakthrough (i.e., effluent concentration equals influent concentration) requires a procedure for standardizing the results.

The method described by Burgisser et al. (1993), hereafter referred to as the "Burgisser Model," provides such a procedure by converting flow through data to sorption isotherms. The Burgisser Model can be used only when dispersion is negligible and local equilibrium is achieved. Local equilibrium is indicated by sorption isotherms which, when superimposed on the same graph, converge on a single sorption isotherm. The Burgisser Model can be used to calculate the mass of metal ion sorbed,  $S$ , based on breakthrough characteristics of a flow through experiment. As in batch tests, the effluent concentration of metal ions,  $C_f$ , can be plotted versus the sorbed concentration,  $S$ , and the Freundlich adsorption coefficients,  $K_f$  and  $n$ , can be determined. Once converted to an adsorption isotherm, the Freundlich equation can be used to calculate the mass of metal ions removed at any effluent concentration, which served as the basis for comparing performance. Flow through results can be compared to batch results by applying the appropriate Freundlich equations, at a selected effluent concentration, and comparing the

mass of metal ions adsorbed,  $S$ . For example, to compare between batch and flow through experiments:

1. Select an effluent concentration,  $C_f$ , for both batch and flow through experiments;
2. Calculate  $S$  for both the batch and flow through experiments from equation 3-5;
3. Compare  $S$  for the different experimental conditions.

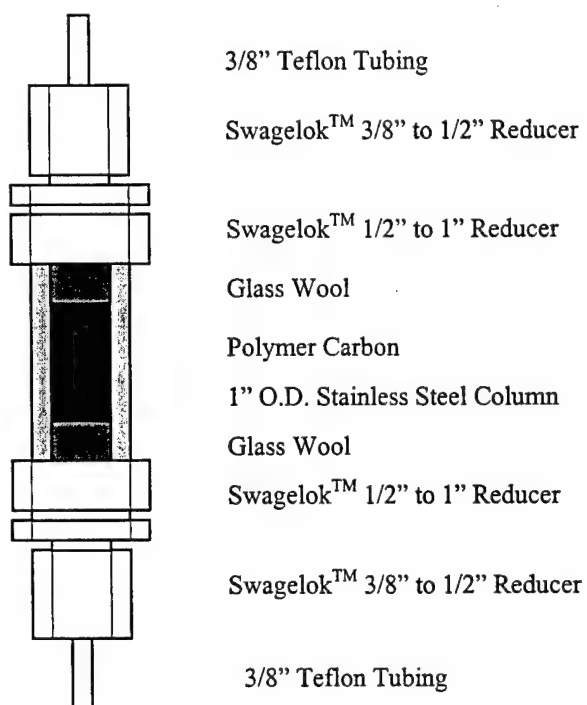


Figure 3-1. Elevation view of a typical adsorbent column (Snoeyink 1990).

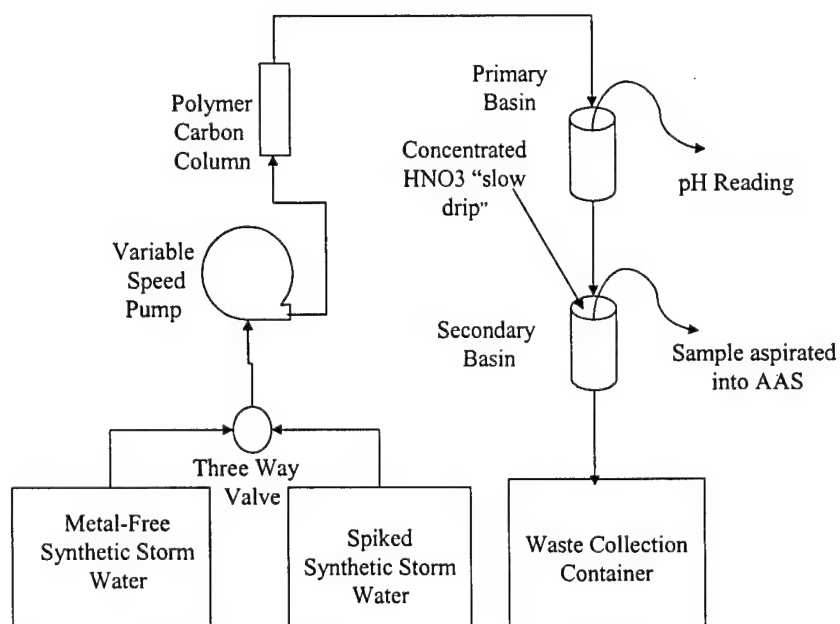


Figure 3-2. Schematic of experimental apparatus for the flow through tests.

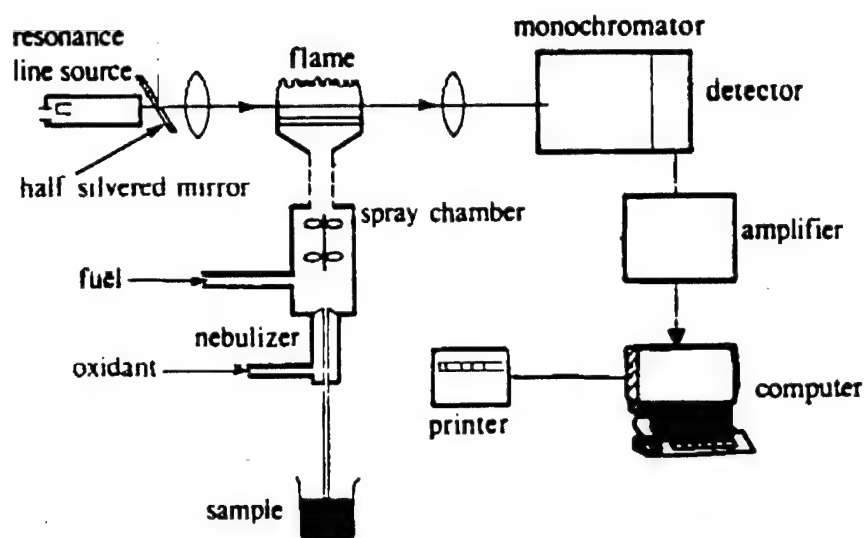


Figure 3-3. Single beam atomic absorption spectrometer (Fifield and Haines 1995).

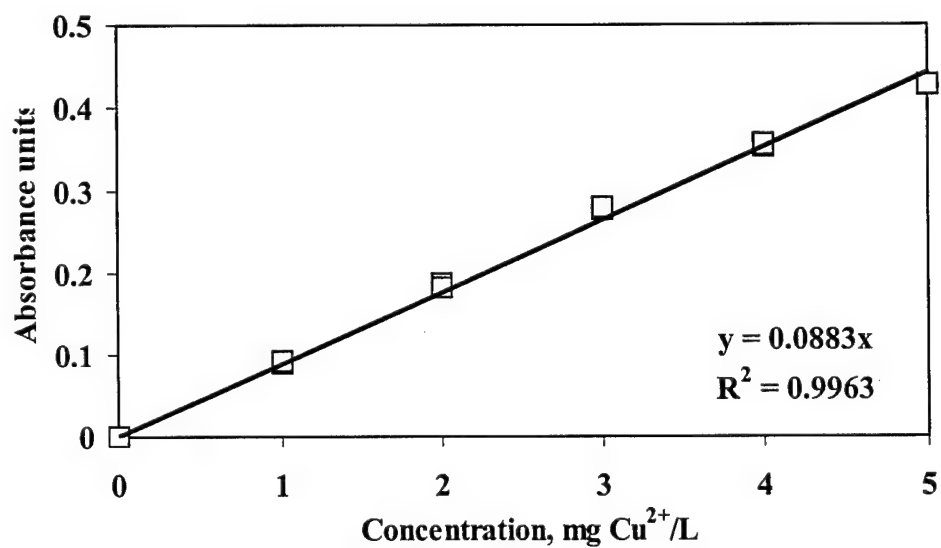


Figure 3-4. Representative AAS calibration curve.

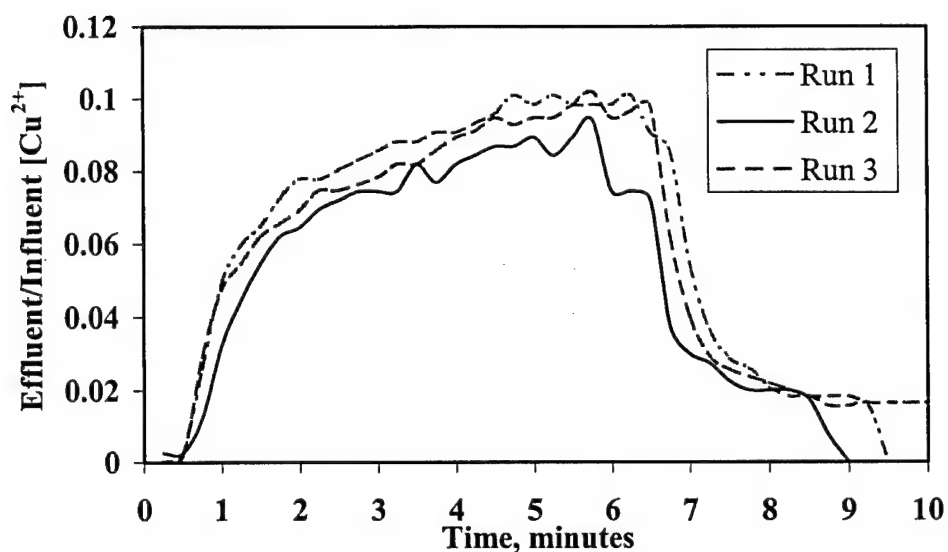


Figure 3-5. Representative time to breakthrough curve. The data shown is the triplicate data set of Supelcarb<sup>TM</sup> at an influent concentration of 5 mg  $\text{Cu}^{2+}$ /L and constant flow rate of 300 mL/min.

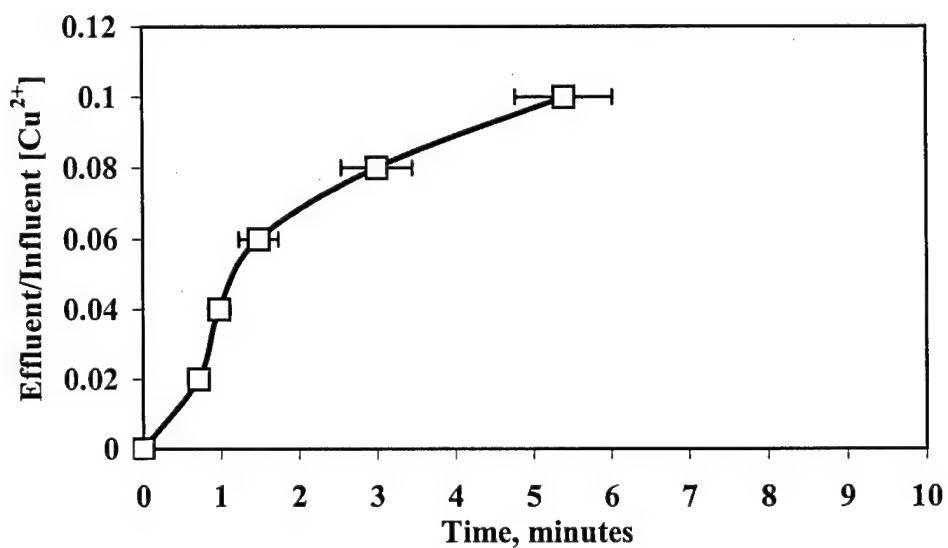


Figure 3-6. Representative average time to breakthrough curve. The graph shows reduction of the triplicate data set of Supelcarb<sup>TM</sup> at an influent concentration of 5 mg  $\text{Cu}^{2+}$ /L and constant flow rate of 300 mL/min to one average break through curve. Error bars represent the standard deviation about the mean time value.



## Chapter 4

### RESULTS AND DISCUSSION

The objective of the experimental portion of this research was to determine the effectiveness of two commercially available charred porous polymers as sorbents for dissolved heavy metals in storm water. The performance of the two charred porous polymers was analyzed under two distinct experimental conditions, batch and flow through. The flow through experiments were further divided into two phases; adsorption of a single dissolved metal and adsorption of two dissolved metals (bislute). Quantitative measurements of the concentrations of dissolved metal(s), in both influent and effluent solutions, were made by AAS.

#### 4.1 Results

##### 4.1.1 $\text{Cu}^{2+}$ in Synthetic Storm Water

###### 4.1.1.1 Batch Results for $\text{Cu}^{2+}$

Results of the batch experiments for  $\text{Cu}^{2+}$  are presented in Figures 4-1 and 4-2. For each charred porous polymer the mass of  $\text{Cu}^{2+}$  sorbed per mass of sorbent is plotted versus the effluent concentration. As discussed in Section 3.3, triplicate tests were conducted on each of eight influent concentrations. The samples were continually mixed for ten minutes. After ten minutes, the samples were filtered, the supernant was acidified with concentrated nitric acid, and the concentration of  $\text{Cu}^{2+}$  in the effluent determined by AAS.

The results indicate total removal of  $\text{Cu}^{2+}$  in influent concentrations of 10 mg/L or less. The convex shape of the data in both figures indicates the Freundlich constant,  $n$ , is less than 1 for both adsorbents (Schwarzenbach, Gschwend, and Imboden 1993), which suggests strong adsorption bonds (Snoeyink 1990).

Figures 4-1 and 4-2 also indicate the adsorption capacities, the maximum amount of metal ions adsorbed for a specific experimental condition, ( $S_{\max}$ ), for each charred porous polymer. Figure 4-1 shows Supelcarb™ with a  $S_{\max}$  of 11 mg  $\text{Cu}^{2+}$ /g adsorbent, while Figure 4-2 shows 12 mg  $\text{Cu}^{2+}$ /g adsorbent for Carboxen-1011™.

Freundlich constants are calculated from the slope, which represents  $n$ , and the y-intercept, representing  $K_f$ , of the plot of the  $\ln$  of the mass  $\text{Cu}^{2+}$  sorbed per gram of adsorbent,  $\ln S$ , versus the  $\ln$  of the effluent concentration,  $\ln C$ . Figure 4-3 represents the plot of  $\ln S$  versus  $\ln C$  for Supelcarb™ and is typical of the method used to calculate Freundlich constants, which are listed in Table 4-1.

Table 4-1. Summary of Freundlich adsorption isotherm coefficients for Supelcarb™ and Carboxen-1011™ from batch experiments with  $\text{Cu}^{2+}$  in synthetic storm water.

Charred Porous Polymer	Freundlich Coefficients	
	$K_f (\text{L/g})^{1/n}$	$n$
Supelcarb™	3.07	0.31
Carboxen-1011™	5.31	0.20

#### **4.1.1.2 Flow Through Experiment Results for $\text{Cu}^{2+}$**

Results of the flow through experiments for  $\text{Cu}^{2+}$  in the synthetic storm water solution are presented in Figures 4-4 through 4-7. For each charred porous polymer, the effluent concentrations, as a percent of the influent concentrations, are plotted versus time. As discussed in Section 3.3, triplicate tests were conducted at each concentration for each flow setting. The results demonstrate that both charred porous polymers effectively remove  $\text{Cu}^{2+}$  from synthetic storm water at low flow rates. Both polymers exhibited approximately linear relationships between effluent concentration and time, above the first measurable  $\text{Cu}^{2+}$  concentration until breakthrough. The results also indicate disproportionate responses to increases in flow, but not to increases in concentration. For example, doubling the flow from 100 mL/min to 200 mL/min, reduced  $\text{Cu}^{2+}$  breakthrough time by 75% to 85%. Doubling the concentration from 2.5 mg  $\text{Cu}^{2+}$ /L to 5 mg  $\text{Cu}^{2+}$ /L reduced  $\text{Cu}^{2+}$  breakthrough time by 10% to 25%.

#### **4.1.1.3 Freundlich Isotherm Coefficients from Flow Through Data for $\text{Cu}^{2+}$**

Results of the flow through experiments for Supelcarb with  $\text{Cu}^{2+}$  in synthetic storm water, integrated to calculate the corresponding sorbed concentration (Burgisser et al. 1993), are presented in Figures 4-8 and 4-9. Figures 4-8 and 4-9 show the sorption isotherms for each experimental influent concentration and flow setting. The figures show the calculated quantities of mass  $\text{Cu}^{2+}$  sorbed,  $S$ , plotted against the corresponding measured effluent concentrations,  $C_f$ .

Since the adsorption isotherms, as calculated by the Burgisser Model do not overlap along a single line, the results indicate non-local equilibrium. Therefore, the

Burgisser Model cannot be used since equilibrium is a requirement for application of the model. The results also indicate both charred porous polymers more effectively removed  $\text{Cu}^{2+}$  at lower flow rates and lower concentrations. The results show rates of removal were reduced as the flow rates or influent concentrations were increased.

#### **4.1.2 $\text{Ni}^{2+}$ in Synthetic Storm Water**

##### **4.1.2.1 Batch Results for $\text{Ni}^{2+}$**

Results of the batch experiments for  $\text{Ni}^{2+}$  in synthetic storm water solution are presented in Figures 4-10 and 4-11. As in Figures 4-1 and 4-2, the mass  $\text{Ni}^{2+}$  per mass of sorbent is plotted, for each charred porous polymer, versus the effluent concentration. The results indicate that these charred porous polymers did not appreciably remove  $\text{Ni}^{2+}$ . Table 4-2 summarizes the Freundlich constants for  $\text{Ni}^{2+}$  in synthetic storm water solution. Figures 4-10 and 4-11 also show  $S_{\text{max}}$  for Supelcarb<sup>TM</sup> of 0.13 mg  $\text{Ni}^{2+}$ /g and 1.8 mg  $\text{Ni}^{2+}$ /g for Carboxen-1011<sup>TM</sup>.

Table 4-2. Summary of Freundlich adsorption isotherm coefficients for Supelcarb<sup>TM</sup> and Carboxen-1011<sup>TM</sup> from batch experiments with  $\text{Ni}^{2+}$  in synthetic storm water.

Charred Porous Polymer	Freundlich Coefficients	
	$K_f(\text{L/g})^{1/n}$	n
Supelcarb <sup>TM</sup>	0.122	0.058
Carboxen-1011 <sup>TM</sup>	0.621	0.270

#### **4.1.2.2 Flow Through Experiment Results for $\text{Ni}^{2+}$**

Results of the flow through experiments for  $\text{Ni}^{2+}$  in synthetic storm water solution are presented in Figures 4-12 and 4-13. For each charred porous polymer, the effluent concentrations, as a percent of the influent concentrations, are plotted versus time. Triplicate tests were conducted at a constant flow rate of 200 mL/min. As with the batch experiments, the charred porous polymers were ineffective at removing  $\text{Ni}^{2+}$  from synthetic storm water.

#### **4.1.3 Competitive Adsorption Flow Through Results for $\text{Cu}^{2+}$ and $\text{Ni}^{2+}$**

Results of the flow through experiments for  $\text{Cu}^{2+}$  and  $\text{Ni}^{2+}$  in the synthetic storm water solution are presented in Figures 4-14 and 4-15. For each charred porous polymer, the effluent concentrations, as a percentage of the influent concentrations, are plotted versus time. The plots show results of the 5 mg  $\text{Cu}^{2+}$ /L at 300 mL/min, without  $\text{Ni}^{2+}$ , for comparison to flow through experiments when  $\text{Ni}^{2+}$  was present. Triplicate tests were conducted at each concentration. All competitive flow through experiments were conducted at a constant flow rate of 300 mL/min. Taking into consideration the results of the  $\text{Ni}^{2+}$  batch and flow through experiments, the tests were run to determine the effect of the presence of the  $\text{Ni}^{2+}$  on  $\text{Cu}^{2+}$  removal.

The results indicate each charred porous polymer responded differently to the presence of a competing cation. Supelcarb™ responded with equal or longer time to breakthrough, while Carboxen-1011™ responded with all shorter breakthrough times.

## **4.2 Discussion**

### **4.2.1 Comparison of Batch to Flow Through Experiments**

Comparing the sorbed mass of  $\text{Cu}^{2+}$  showed both charred porous polymers achieved much higher removal capacity in batch experiments than flow through tests. Contact time between the solute and the charred porous polymers in batch experiments ranged from 40 to 115 times greater than flow through experiments. The lowest flow through mass flow rates displayed adsorption capacities between one-thirtieth and one-tenth of the capacities observed in batch experiments. The results indicate removal effectiveness is a function of the residence time of the solute in the adsorbent bed.

Figures 4-4 through 4-7 show both charred porous polymers demonstrated approximately linear characteristics from the first measurable  $\text{Cu}^{2+}$  in the effluent, until the concentration reached breakthrough. The significant difference between the charred porous polymers is the lag time from the start of the experiment until the effluent concentration reached 2% of the influent. This lag time represents the depth of the bed over which the concentration changes from the influent value to zero. The column depth over which this occurs is referred to as the mass transfer zone (Freeman 1989). Carboxen-1011™ demonstrated a consistently longer mass transfer zone than Supelcarb™.

Two interesting observations result from increasing the flow rates. First, the time for the influent to cross the mass transfer zone shortens disproportionately to the increase in fluid velocity. For example, doubling the flow rate, from 100 to 200 mL/min, reduced the time for  $\text{Cu}^{2+}$  to cross the mass transfer zone by 85 to 90%. Tripling the flow rate,

from 100 to 300 mL/min, produced nearly identical results with the time  $\text{Cu}^{2+}$  to cross the mass transfer zone reduced by approximately 95%. The second observation is that as flow rates increased, Carboxen-1011<sup>TM</sup> exhibited an approximately constant rate of increase in effluent concentrations. In contrast, Supelcarb<sup>TM</sup> demonstrated an overall-increasing rate of concentration change.

Increasing  $\text{Cu}^{2+}$  concentrations, while maintaining constant flow rate, indicated a shorter time to cross the mass transfer zone. Overall, Supelcarb<sup>TM</sup> responses to increased  $\text{Cu}^{2+}$  concentrations indicated constant relationships between increases in the mass flow rate and the time to reach a specific effluent concentration. For example, doubling the concentration from 2.5 mg  $\text{Cu}^{2+}$ /L to 5 mg  $\text{Cu}^{2+}$ /L resulted in an approximately 75% reduction in time to reach each effluent concentration. The Carboxen-1011<sup>TM</sup> responded to increased concentrations with nearly identical times for the medium and high concentrations of  $\text{Cu}^{2+}$  to cross the mass transfer zone, both of which were approximately half the time for the low concentration.

Once through the mass transfer zone, Carboxen-1011<sup>TM</sup> exhibited nearly identical responses to the low and intermediate concentrations. The response to high influent concentration appeared to be a constant proportion, approximately 50%, of the low concentration. Carboxen-1011<sup>TM</sup> demonstrated longer times to cross the mass transfer zone than Supelcarb<sup>TM</sup> for the low and intermediate concentrations and approximately identical response to the high concentration.

The adsorption isotherms calculated by the Burgisser Model (Figures 4-8 and 4-9), demonstrated that an experimental equilibrium was not achieved. Had the experiment

reached equilibrium the adsorption isotherms would have overlapped and appeared as a single line. Experimental equilibrium is a requirement for the Burgisser Model, and therefore is no longer applicable.

Overall, the comparison of the mass of  $\text{Cu}^{2+}$  sorbed for flow through experiments and batch experiments showed decreasing removal capacity as mass flow rates increased and hydraulic residence times decreased.

#### **4.2.2 Comparison of Adsorption of $\text{Cu}^{2+}$ to $\text{Ni}^{2+}$**

Neither adsorbent was effective in removing  $\text{Ni}^{2+}$ . Both adsorbents displayed mass transfer times below 30 seconds and breakthrough times less than one minute. Both porous polymers adsorbed 100 to 200 times more  $\text{Cu}^{2+}$  than  $\text{Ni}^{2+}$ .

#### **4.2.3 Comparison of Adsorption of $\text{Cu}^{2+}$ as a single solute to a bisolute system with $\text{Ni}^{2+}$ present**

The presence of  $\text{Ni}^{2+}$  had noticeably different effects on the removal of  $\text{Cu}^{2+}$  by the two charred porous polymers. At equi-molar concentrations of  $\text{Cu}^{2+}$  and  $\text{Ni}^{2+}$ , Supelcarb™ demonstrated an order of magnitude increase in mass  $\text{Cu}^{2+}$  removed compared to the similar test condition, 5 mg  $\text{Cu}^{2+}$ /L at 300 mL/min, with  $\text{Cu}^{2+}$  as a single solute. At other molar ratios,  $2\text{Cu}^{2+}:1\text{Ni}^{2+}$  and  $1\text{Cu}^{2+}:2\text{Ni}^{2+}$ , there is no clearly discernable difference in the mass of  $\text{Cu}^{2+}$  removed by Supelcarb™ when  $\text{Ni}^{2+}$  was present, compared to the condition when  $\text{Cu}^{2+}$  was present as a single solute. Mass of  $\text{Cu}^{2+}$  sorbed by Carboxen-1011™ showed an insignificant variation between the single solute and equi-molar bisolute experiments. The remaining bisolute conditions showed slightly less and approximately equal  $\text{Cu}^{2+}$  removal by Carboxen-1011™.



The results fail to indicate governing relationships between the presence of a competing cation and removal of  $\text{Cu}^{2+}$  by charred porous polymers. However, it is significant to note that removal of  $\text{Cu}^{2+}$  by Supelcarb<sup>TM</sup> either equaled or increased when  $\text{Ni}^{2+}$  was present while removal of  $\text{Cu}^{2+}$  by Carboxen-1011<sup>TM</sup> equaled or decreased under similar conditions.

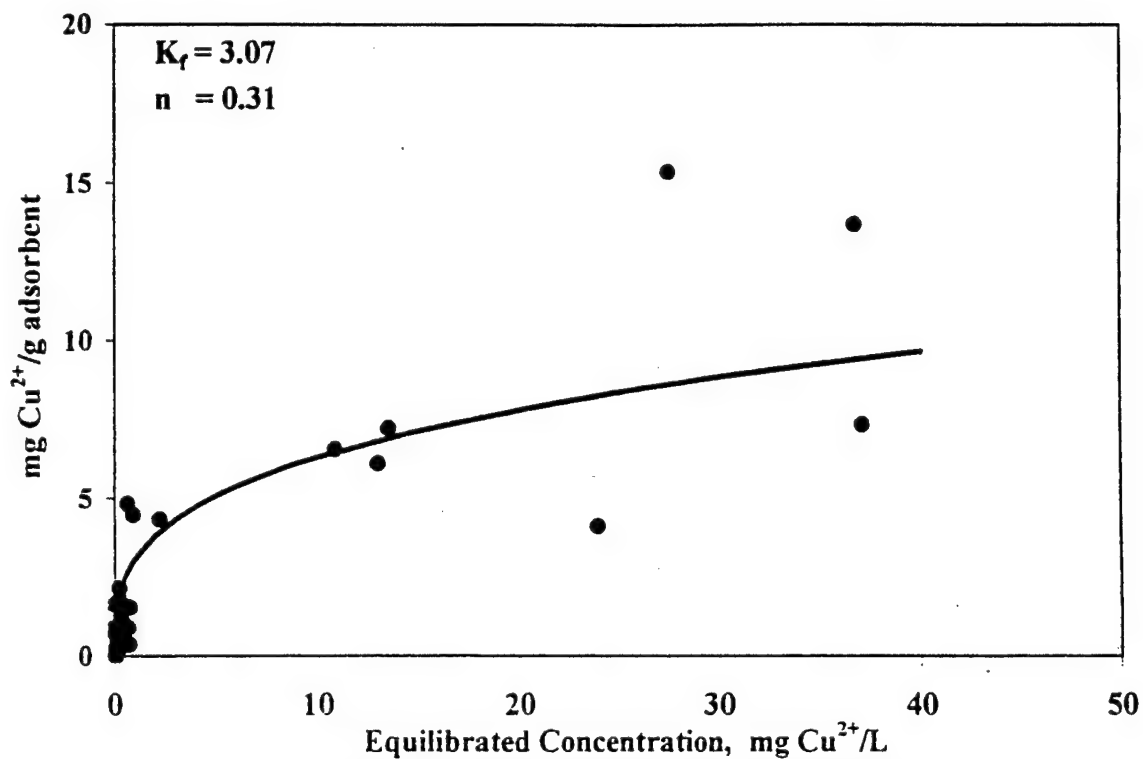


Figure 4-1. Copper adsorption isotherm obtained with Supelcarb<sup>TM</sup> in the batch experiments.

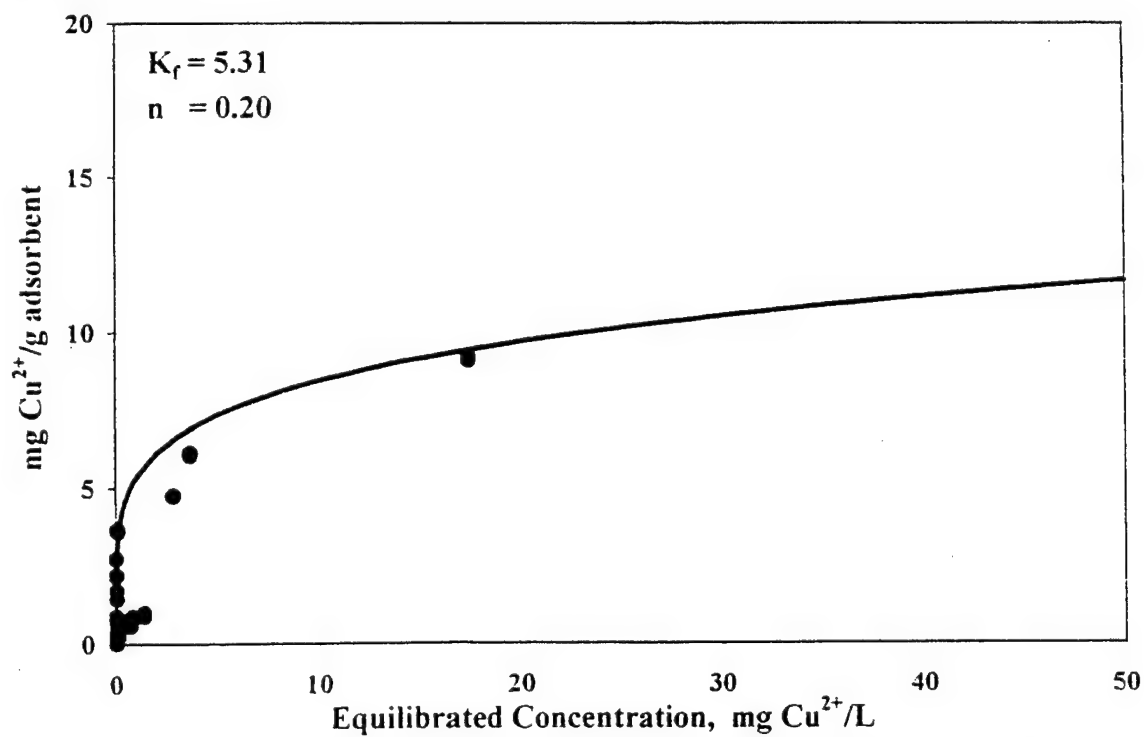


Figure 4-2. Copper adsorption isotherm obtained with Carboxen-1011<sup>TM</sup> in the batch experiments.

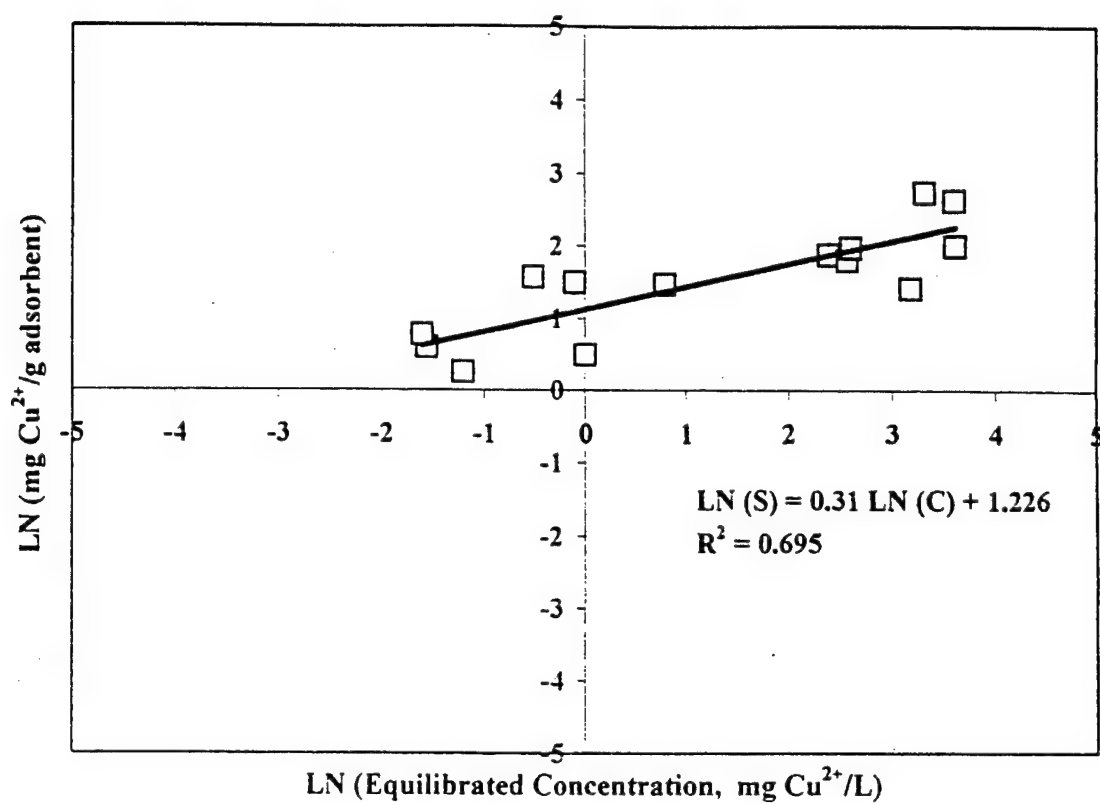


Figure 4-3. Fruendlich adsorption isotherm obtained with Supelcarb<sup>TM</sup> in the batch experiments.

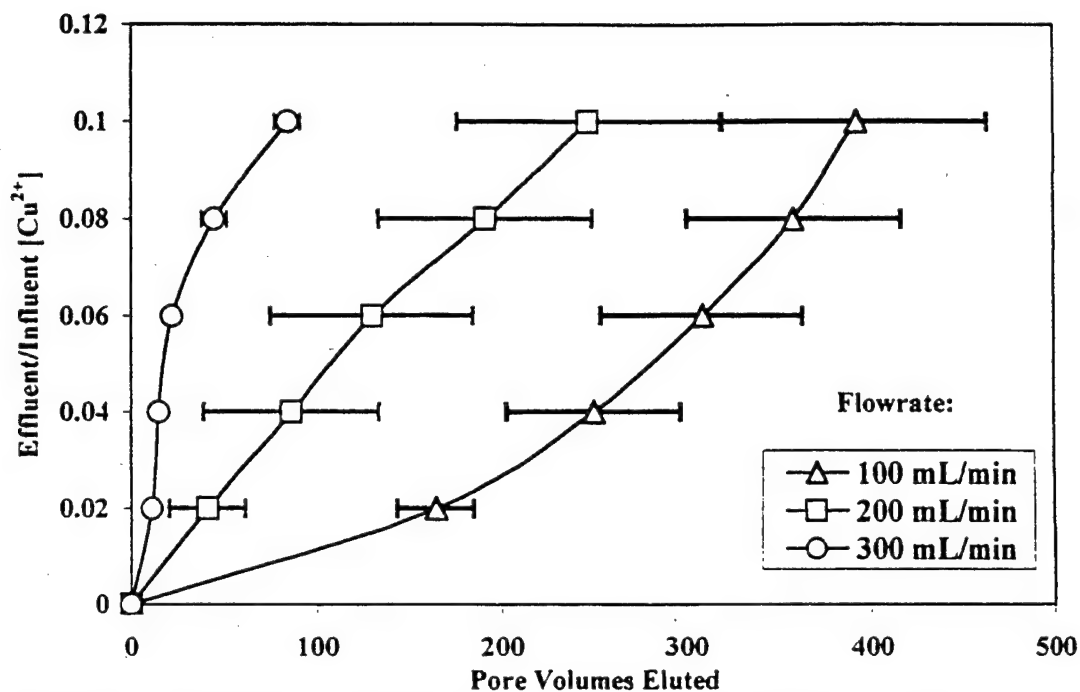


Figure 4-4. Copper breakthrough curves obtained with Supelcarb™ and a constant influent concentration of 5 mg Cu<sup>2+</sup>/L in the flow through experiments. Error bars represent a standard deviation about a triplicate mean.

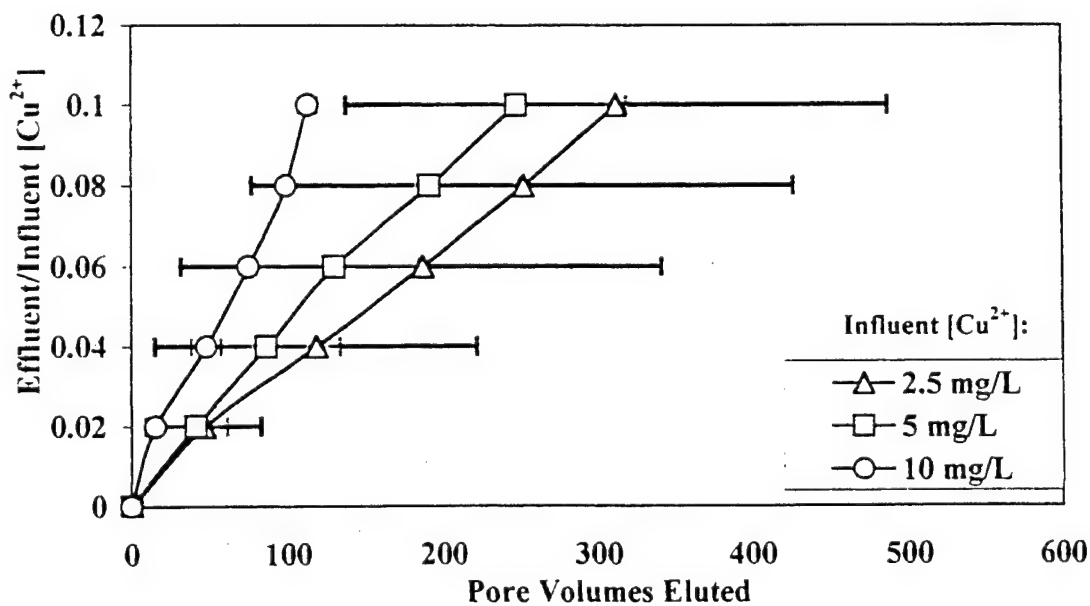


Figure 4-5. Copper breakthrough curves obtained with Supelcarb™ and a constant flow rate of 200 mL/min in the flow through experiments. Error bars represent a standard deviation about a triplicate mean (10 mg Cu<sup>2+</sup>/L error bars no larger than symbol size).

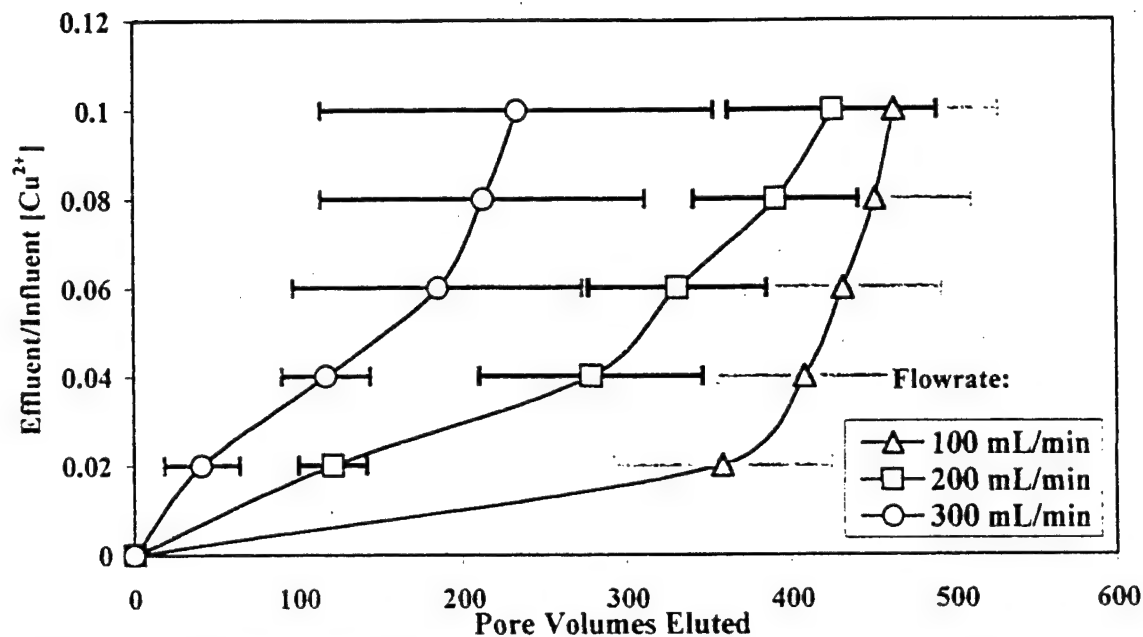


Figure 4-6. Copper breakthrough curves obtained with Carboxen-1011<sup>TM</sup> and a constant influent concentration of 5 mg Cu<sup>2+</sup>/L in the flow through experiments. Error bars represent a standard deviation about a triplicate mean.

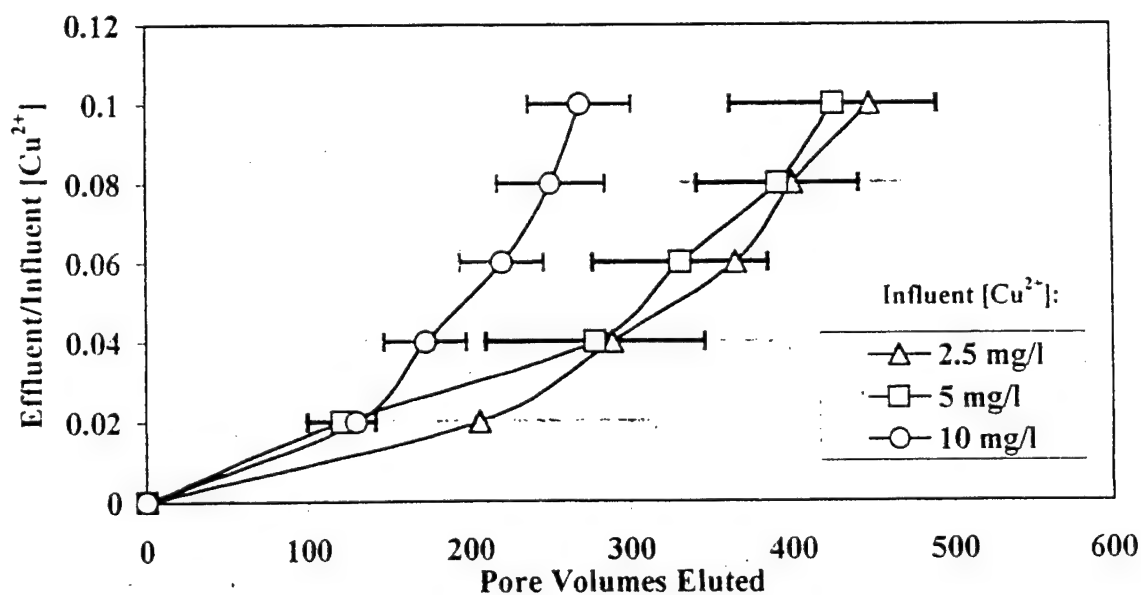


Figure 4-7. Copper breakthrough curves obtained with Carboxen-1011<sup>TM</sup> and a constant flow rate of 200 mL/min in the flow through experiments. Error bars represent a standard deviation about a triplicate mean.

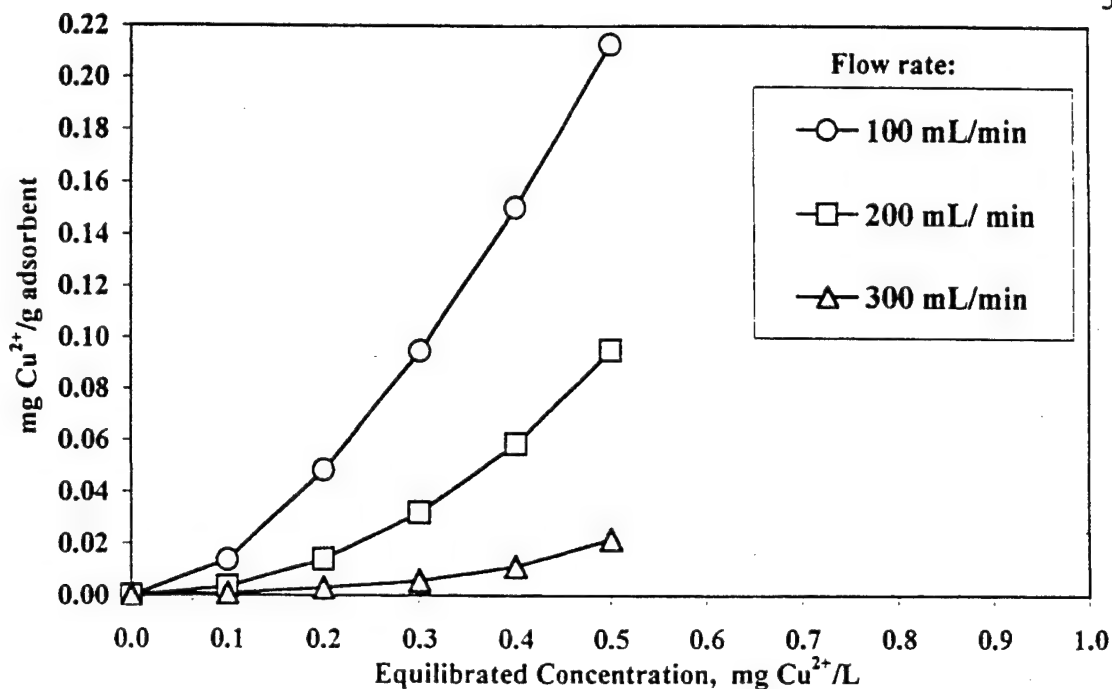


Figure 4-8. Adsorption isotherms obtained with Supelcarb™ as calculated by the Burgisser Model for a constant influent concentration of  $\text{Cu}^{2+}$  of 5 mg  $\text{Cu}^{2+}$ /L in the flow through experiments.

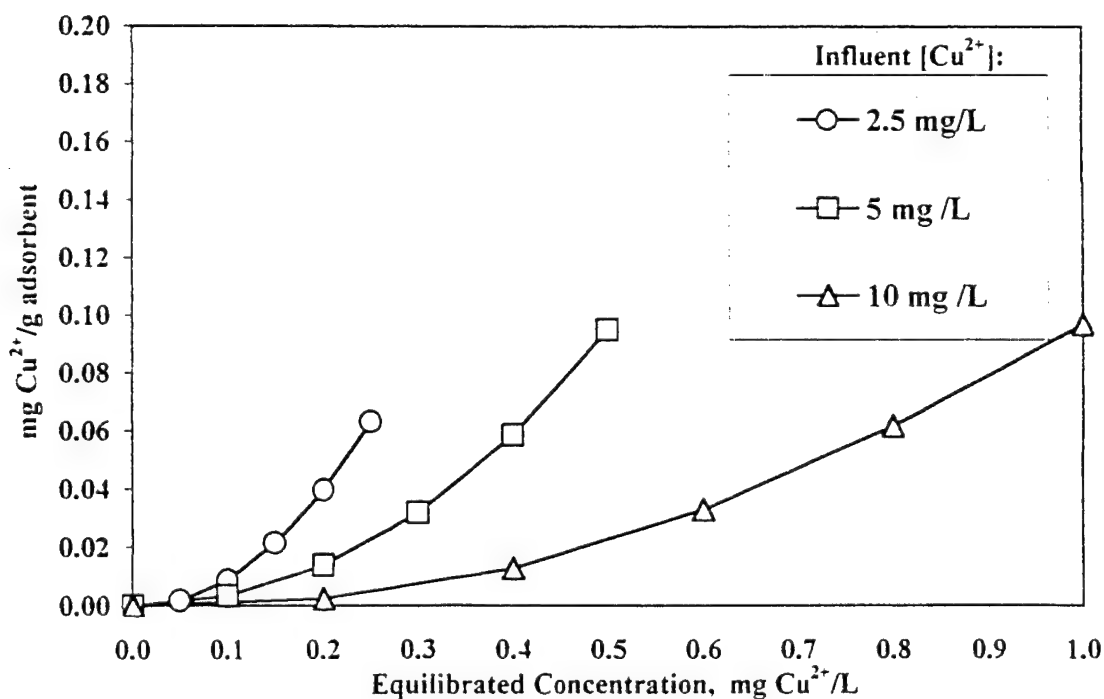


Figure 4-9. Adsorption isotherms obtained with Supelcarb™ as calculated by the Burgisser Model for a constant flow rate of 200 mL/min in the flow through experiments.

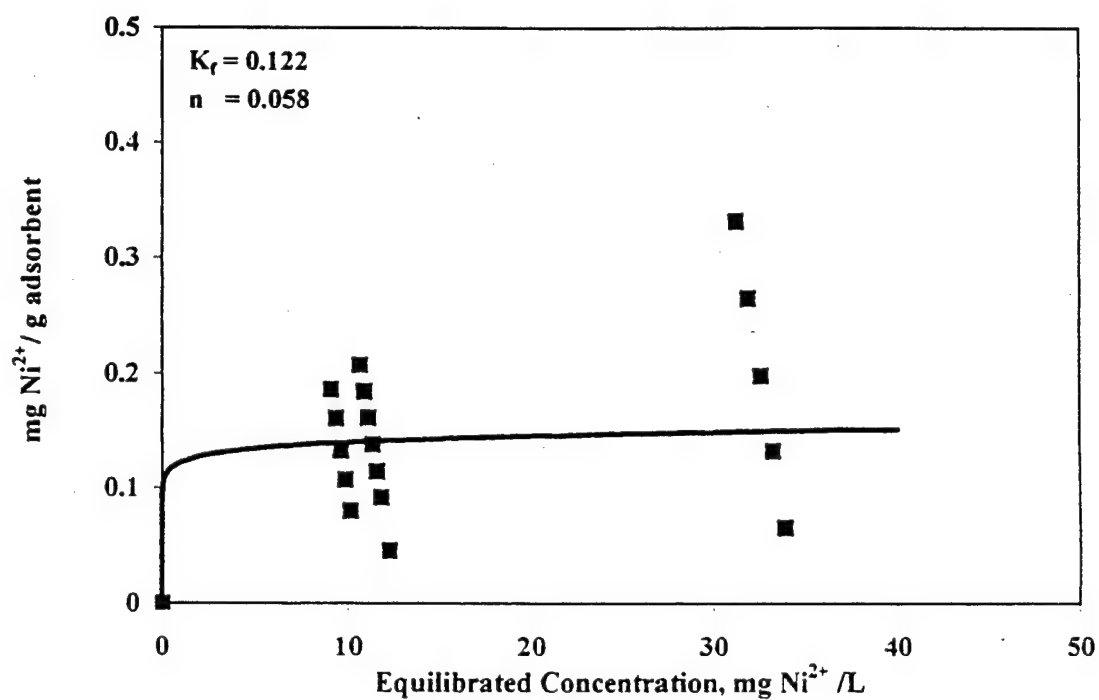


Figure 4-10. Nickel adsorption isotherm obtained with Supelcarb™ in the batch experiments.

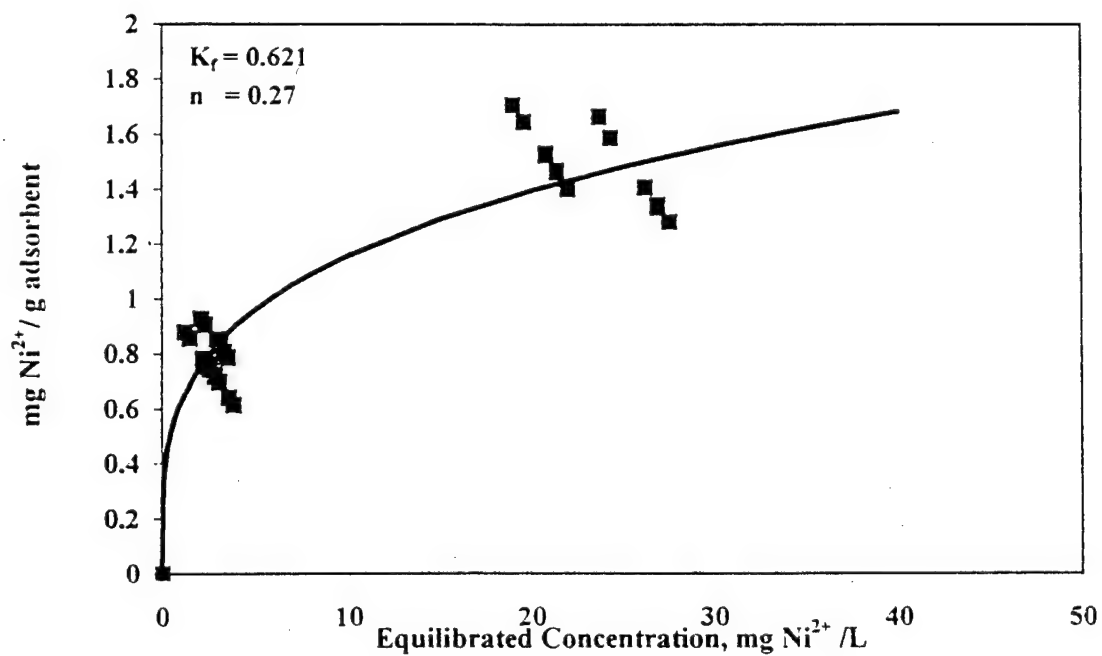


Figure 4-11. Nickel adsorption isotherm obtained with Carboxen-1011™ in the batch experiments.

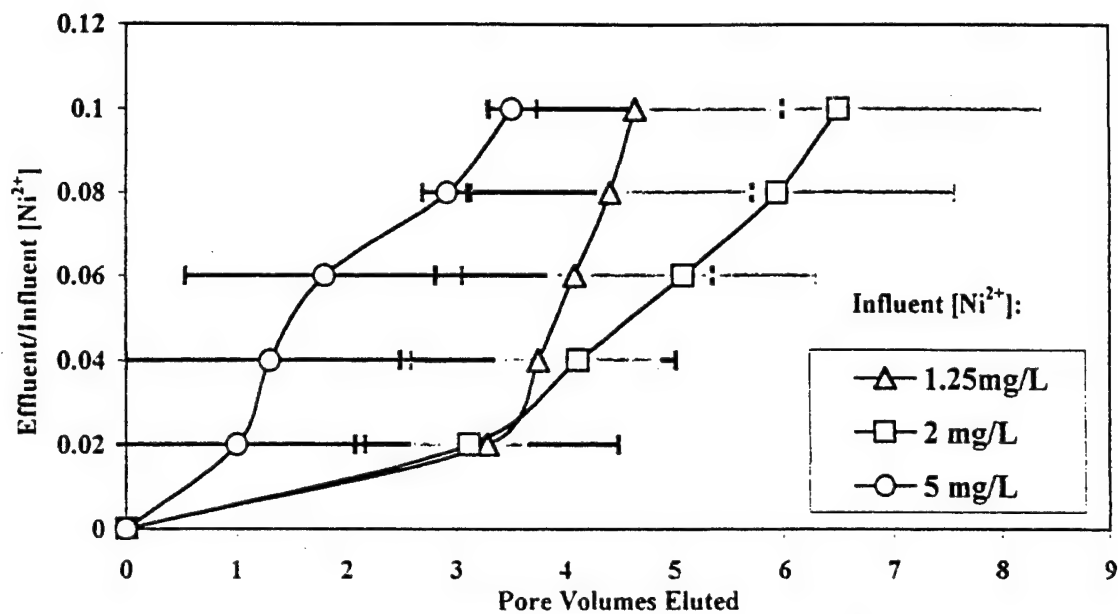


Figure 4-12. Nickel breaththrough curves obtained with Supelcarb™ and a constant flow rate of 200 mL/min in the flow through experiments. Error bars represent a standard deviation about a triplicate mean.

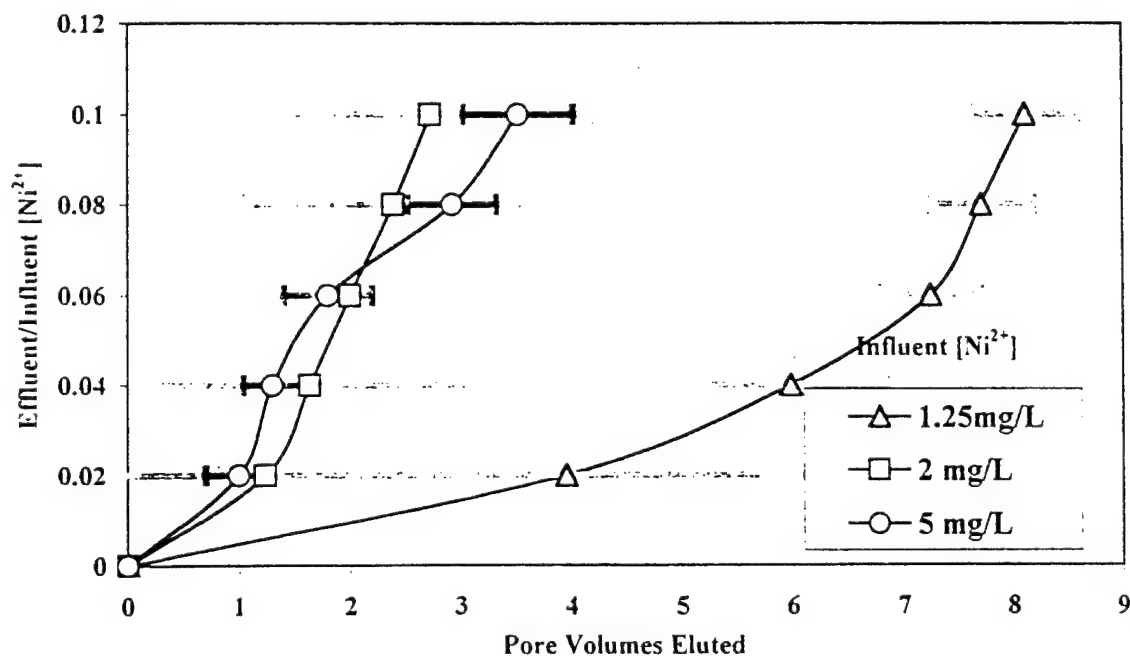


Figure 4-13. Nickel breaththrough curves obtained with Carboxen-1011™ and a constant flow rate of 200 mL/min in the flow through experiments. Error bars represent a standard deviation about a triplicate mean.



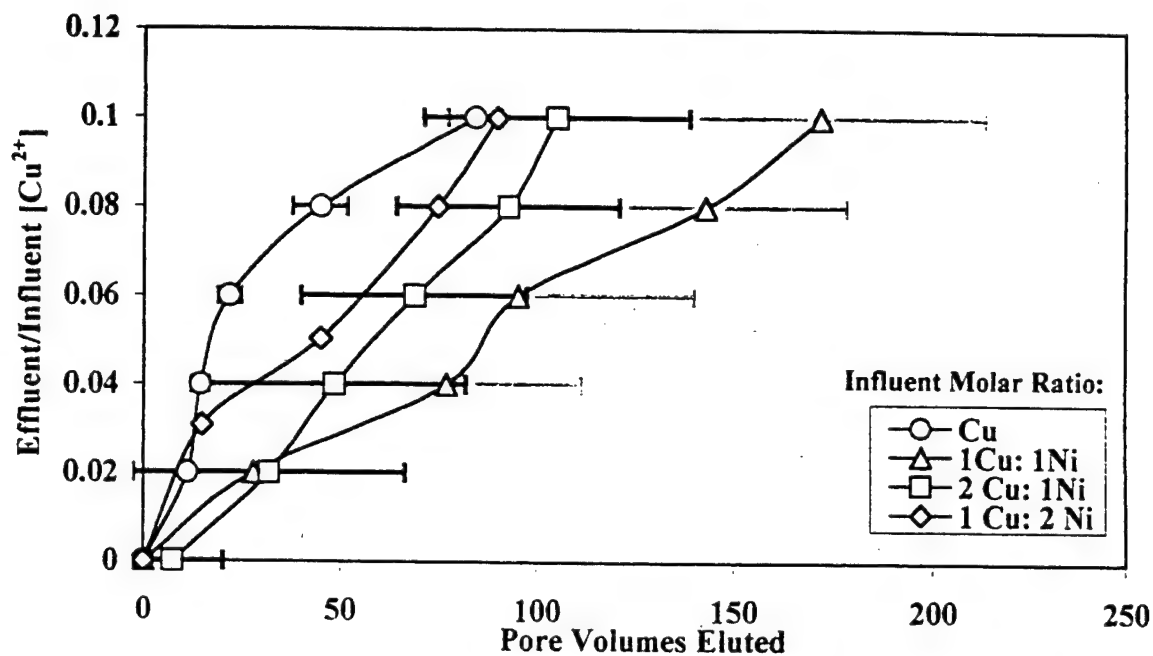


Figure 4-14. Copper breakthrough in a  $Cu^{2+}$  and  $Ni^{2+}$  bisolute system. Curves obtained with Supelcarb<sup>TM</sup> and a constant flow rate of 300 mL/min in the flow through experiments. Error bars represent a standard deviation about a triplicate mean.

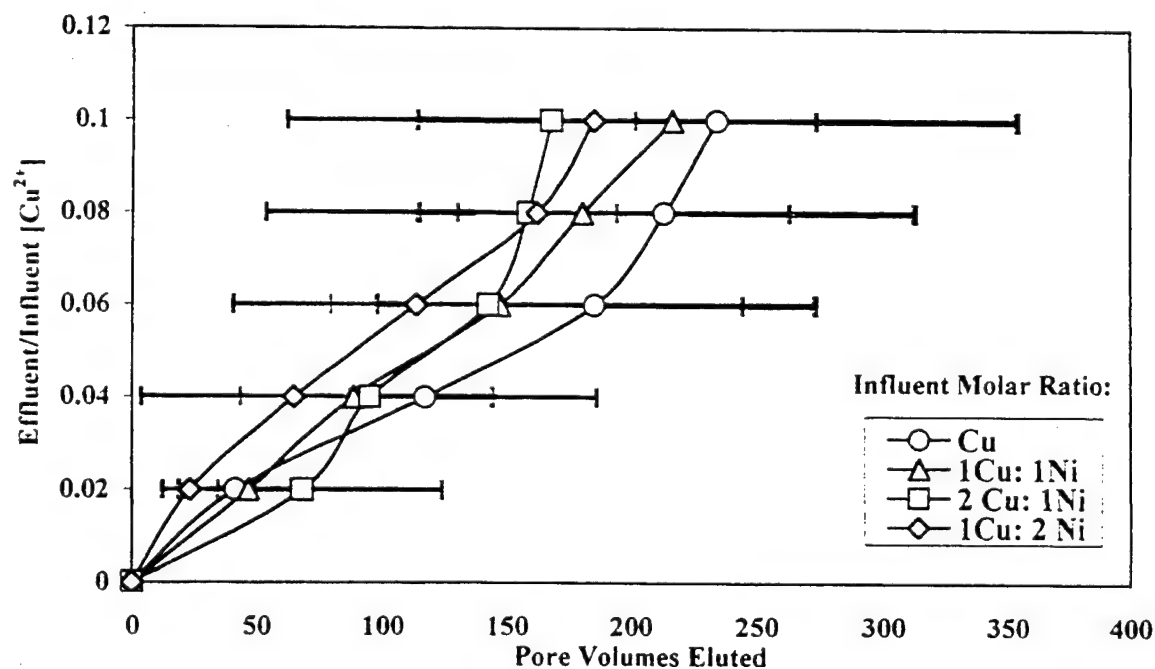


Figure 4-15. Copper breakthrough in a  $Cu^{2+}$  and  $Ni^{2+}$  bisolute system. Curves obtained with Carboxen-1011<sup>TM</sup> and a constant flow rate of 300 mL/min in the flow through experiments. Error bars represent a standard deviation about a triplicate mean.

## Chapter 5

### CONCLUSION

The objectives of this research were to evaluate two commercially available carbonaceous adsorbents for removal of heavy metals from storm water and to determine the feasibility of placing a porous adsorbent within a storm water collection system.

Both charred porous polymer adsorbents demonstrated a penchant for removing  $\text{Cu}^{2+}$  from storm water. However, the ability to sorb  $\text{Cu}^{2+}$  decreased significantly as either the fluid velocity through the adsorbent bed or concentration of  $\text{Cu}^{2+}$  in the influent increased. In contrast,  $\text{Ni}^{2+}$  was not appreciably removed under any experimental condition performed during this research. The presence of a second metal solute,  $\text{Ni}^{2+}$ , did not generally affect removal of  $\text{Cu}^{2+}$ . These charred porous polymers have shown they are not "universally" effective as heavy metal adsorbents. It can therefore be concluded that the charred porous polymers evaluated herein may have only selective applications in environs where the solute species and mass flow rates are known.

Commercially available storm water treatment systems, such as those manufactured by Stormceptor<sup>TM</sup> and Vortech<sup>TM</sup>, have been shown to be practical components for the placement of a cartridge of adsorbent material. These treatment systems have the sediment removal, high-flow bypass capabilities, and accessibility that would make attaching a replaceable sorbent cartridge feasible.

In summary, while the concept of placing a replaceable cartridge of sorbent material has a broad range of potential applications and merits further consideration, selection of the sorbent material requires evaluation based on site specific effluent characteristics.

## BIBLIOGRAPHY

- Adams, T. L., R. C. Anderson, F. W. Brownell, D. R. Case, L. M. Gallagher, W. T. Halbleid, S. W. Landfair, R. T. Lee, M. L. Miller, K. J. Nardi, A. P. Olney, J. M. Scagnelli, J. W. Spensley, T. F. P. Sullivan, S. E. Williams. Environmental Law Handbook. 14<sup>th</sup> ed. Rockville, MD: Government Institutes, Inc., 1997.
- Allen, S. J. Types of Adsorbent Materials. In Adsorbents McKay (ed.) (pp.59 – 97). New York: CRC Press, 1996.
- American Public Health Association, American Water Works Association, Water Pollution Control Federation. Standard Methods for Examination of Water and Wastewater. 16<sup>th</sup> ed. Edited by Mary Ann H. Franson. Washington, D.C.: American Public Health Association, 1985.
- Applied Research Laboratory, Pennsylvania State University, Survey of Air and Water Quality Pollution Prevention and Control Technology Used in Shipyards and Similar Industries: a report for the National Shipbuilding and Research Program (NSRP). State College, PA: 1997.
- Burgisser, Christa S., Miroslav Cernik, Michal Borkovec, and Hans Sticher. "Determination of Nonlinear Adsorption Isotherms from Column Experiments: An alternative to Batch Studies." Environmental Science and Technology. Vol. 27. No. 5 (1993): 943-948.
- Burgos, W.D., and Alexander Ellwood. "Regulatory Methods used in Writing NPDES Permits for the Shipbuilding and Repair Industry." Journal of Environmental Management. To be published.
- Dodson, R. D. Storm Water Pollution Control: Industry and Construction NPDES Compliance. New York: McGraw-Hill, Inc., 1995.
- Faust, Samuel D., and Osman M. Aly. Adsorption Processes for Water Treatment. Boston: Butterworth, 1987.
- Fifield, F. W., and P. J. Haines, ed. Environmental Analytical Chemistry. London: Blackie Academic & Professional, 1995.
- Foran, Jeffrey A. Regulating Toxic Substances in Surface Water. Boca Raton, FL: Lewis Publishers, 1993.

- Freeman, Harry M., Editor-in-chief. Standard Handbook of Hazardous Waste Treatment and Disposal. New York: McGraw-Hill, Inc., 1989.
- Gadboise, L. E. Reconnaissance Sampling at an Arid Navy Base. Naval Command, Control and Ocean Surveillance Center, San Diego: 1997.
- Gauthier, R. C., S. J. Harrell, R. K. Johnston, G. S. Key, P. J. Earley, M. Caballero. An Integrated Marine Environmental Compliance Program for Naval Shipyards: Phase I Report. San Diego: NRAD, 1995. Prepared for Naval Sea Systems Command.
- Gauthier, R. D., J. T. Gilchrest, G. S. Key, P. J. Earley, A. O. Valkers, H. Tees, D. Sutton. An Integrated Marine Environment Compliance Program for Naval Shipyards: Phase II/II. San Diego: NraD, 1996. Prepared for Naval Sea Systems Command.
- Hartman Engineering Inc, Avondale Industries, Inc., and Walk, Haydel Environmental. Impacts on Shipyards from Reauthorization of the Federal Clean Water Act. prepared for the National Steel and Shipbuilding Company. San Diego: 1997.
- Host, Philip. "Dry Dock Water Pollution Control Efforts at Norfolk Naval Shipyard." Naval Engineer's Journal (March 1996):57-64.
- LaGrega, M. D., P. L. Buckingham, and J. C. Evans. Hazardous Waste Management. New York: McGraw-Hill, 1994.
- Liu, Kuang-Tsan and Walter J. Weber, Jr. "Characterization of Mass Transfer Parameters for Adsorber Modeling and Design". Journal Water Pollution Control Federation, Vol. 53. No. 10. (October 1981): 1541-1548.
- Manning, C. J. "Analysis of Pollution Prevention Efforts for Ships Homeported at Norfolk Naval Base, Norfolk, Virginia." Masters Project, 1995.
- Moore, J. W., and S. Ramamoorthy. Heavy Metals in Natural Waters. New York: Springer-Verlag, 1984.
- Ong, H. Ling and Vernon E. Swanson. "Adsorption of Copper by Peat, Lignite, and Bituminous Coal." Economic Geology, Vol. 61. No. 5. (1966): 1214-1231.
- Puget Sound Naval Shipyard. Best Management Practices Plan. Enclosure (1) to NAVSHIPYDPUGETINST P5090.30A.
- Ross, Jonathon. "Environmental Pollution Control: Regulatory Considerations and a Case in Point." Journal of Ship Production, Vol. 9. No. 3. (August 1993): 159-166.

- Sag, Y. and T. Kutsal. "Copper (II) and Nickel (II) Adsorption by *Rhizopus arrhizus* in Batch Stirred Reactors in Series." The Chemical Engineering Journal. Vol. 58. (1995): 265-273.
- Schnoor, Jerald L. Environmental Modeling Fate and Transport of Pollutants in Water, Air, and Soil. New York: John Wiley & Sons Inc., 1996.
- Schwarzenbach, Rene P., Philip M. Gschwend, and Dieter Imboden. Environmental Organic Chemistry. New York: John Wiley & Sons Inc., 1993.
- Snoeyink, Vernon L., and David Jenkins. Water Chemistry. New York: John Wiley & Sons Inc., 1980.
- Snoeyink, Vernon L. Adsorption of Organic Compounds. In F. W. Pontius (Ed.), Water Quality and Treatment: A Handbook of Community Water Supplies (4<sup>th</sup> ed.) (pp. 781 – 875). New York: McGraw-Hill, 1990.
- Stormceptor Corporation. Stormceptor™ Technical Manual. 1996.
- Vortechnics Corporation. Vortechnics™ Website@www.vortechnics.com. 1998